

The Nainital-Cape Survey-III : A Search for Pulsational Variability in Chemically Peculiar Stars[★]

S. Joshi¹, D. L. Mary², N. K. Chakradhari³, S. K. Tiwari¹, C. Billaud²

¹ Aryabhata Research Institute of Observational Sciences (ARIES), Manora Peak, Nainital, India
e-mail: santosh@aries.res.in

² Université de Nice Sophia Antipolis, Observatoire de la Côte d'Azur, Nice, France
e-mail: david.mary@unice.fr, camille.billaud@wanadoo.fr

³ School of Studies in Physics and Astrophysics, Pt. Ravishankar Shukla University, Raipur, India
e-mail: nkchakradhari@gmail.com

Received; accepted

ABSTRACT

Context. The Nainital-Cape survey is a dedicated research programme to search and study pulsational variability in chemically peculiar stars in the Northern Hemisphere.

Aims. The aim of the survey is to search such chemically peculiar stars which are pulsationally unstable.

Methods. The observations of the sample stars were carried out in high-speed photometric mode using a three-channel fast photometer attached to the 1.04-m Sampurnanand telescope at ARIES.

Results. The new photometric observations confirmed that the pulsational period of star HD 25515 is 2.78-hrs. The repeated time-series observations of HD 113878 and HD 118660 revealed that previously known frequencies are indeed present in the new data sets. We have estimated the distances, absolute magnitudes, effective temperatures and luminosities of these stars. Their positions in the H-R diagram indicate that HD 25515 and HD 118660 lie near the main-sequence while HD 113878 is an evolved star. We also present a catalogue of 61 stars classified as null results, along with the corresponding 87 frequency spectra taken over the time scale 2002-2008. A statistical analysis of these null results shows, by comparison with past data, that the power of the noise in the light curves has slightly increased during the last few years.

Key words. stars: chemically peculiar – stars: oscillations – stars: variables – stars: roAp – stars: δ -Scuti: individual (HD 25515 – HD 113878 – HD 118660)

1. Introduction

A survey project called “Nainital-Cape Survey” was initiated in 1997 between the Aryabhata Research Institute of Observational Sciences (ARIES), Nainital, and the South African Astronomical Observatory (SAAO), Capetown, to search and study the pulsational variability in chemically peculiar (CP) A-F stars. The atmospheres of these stars have an inhomogeneous distribution of chemical elements which are frequently seen as abundance spots on stellar surfaces and as clouds of chemical elements concentrated at certain depths along the stellar radii (see, for example, Kochukhov et al. 2004a; 2004b; Lueftinger et al. 2003; Ryabchikova et al. 2006; 2005; 2002). The inhomogeneity with high abundance gradients is explained by microscopic radiative diffusion processes depending on the balance between gravitational pull and uplift by the radiation field through absorption in spectral lines (Michaud 1970, Michaud et al. 1981; LeBlanc & Monin 2009). Therefore, the CP stars are excellent test objects for astrophysical processes like diffusion, convection, and stratification in stellar atmospheres in the presence of rather strong magnetic fields.

A class of CP (CP2) stars known as Ap (A-peculiar) stars, which rotate considerably more slowly than spectroscopically

normal main sequence stars have similar effective temperatures, strong magnetic fields, normal or below-solar concentrations of light and iron-peak elements, and overabundances of rare Earth elements. A fraction of cool Ap stars in the effective temperature range of ≈ 6400 to 8100 K (Kochukhov & Bagnulo 2006) exhibit anomalously strong Sr, Cr and Eu lines coupled with high-magnetic fields from few to as high as 24.5 kGauss (Kurtz et al. 2006b). Those stars which pulsate in the period of range 5.65 to 22 -min (Kreidl 1985, Kochukhov 2008a), with photometric amplitude variations less than 10 milli-magnitude (mmag) in Johnson B filter, and spectroscopic radial velocity variations of 0.05 to 5 -kms⁻¹ are termed rapidly oscillating Ap (roAp) stars. The roAp pulsations are attributed to low-order ($l < 3$), high-overtones ($n \gg l$), non-radial p -modes and are classically explained by the oblique pulsator model (Kurtz 1982). This model supposes the pulsation axis is aligned to the magnetic axis which is oblique to the rotation axis. As the star rotates the variations in the pulsational amplitude can be observed by a distant observer. Recent theoretical studies of roAp stars show that the axis of the p -mode pulsations is not exactly aligned with the magnetic field because of the centrifugal force (Bigot & Dziembowski 2002). Excitation of pulsations in roAp stars is governed by κ -mechanism acting in the H I ionization zone, with the additional influence from the magnetic quenching of convection and composition gradients built up by the atomic diffusion (Balmforth et al. 2001; Cunha 2002; Vauclair & Théado 2004). These magneto-acoustic pulsators provide a unique op-

Send offprint requests to: Santosh Joshi

[★] Table 7, Figure 11 and Figure 12 are only available in electronic form at <http://www.edpsciences.org>

portunity to study the pulsations in the presence of chemical inhomogeneities and strong magnetic fields.

Apart from the roAp stars, another class of CP stars (CP1) known as Am (A-metallic) stars and preferably found within close binary systems, exhibit low-rotational velocities, lack of magnetic fields, apparent underabundance of calcium and scandium, and overabundance of Fe-peak elements. The former near exclusion between pulsational variability and Am-type chemical peculiarity has evolved considerably in the recent years, and this dichotomy is no longer a clear-cut. Indeed, pulsations of the δ -Scuti type¹ have been evidenced in many Am stars (e.g. Kurtz 1989; Martínez et al. 1999; Kurtz & Martínez 2000; Joshi et al. 2003, González et al. 2008), but our understanding of the physics of pulsating Am stars is still far from being complete. Theoretical models can for instance partially explain that evolved Am stars can pulsate (κ -mechanism in He II can drive the pulsations in evolved Am stars) and that marginal Am stars can be low-amplitude δ -Scuti stars (a sufficient amount of He remains to drive low-amplitude oscillations). However, less well understood are the mechanisms of pulsations in classical Am stars (Kurtz & Martínez 2000), δ -Scuti type pulsations in Ap stars (González et al. 2008), origin of the abundance anomalies either from a superficial or from a much deeper mixing zone (LeBlanc et al. 2008, 2009), co-existence of δ -Scuti and γ -Doradus type pulsations in Am stars (King et al. 2006; Henry & Fekel 2005), limits where chemical peculiarity and pulsations can coexist and where they are mutually exclusive (Hekker et al. 2008) and possible excitation of solar like oscillations in Am stars (Carrier et al. 2007).

The rich pulsation spectra of roAp and pulsating Am stars does not only help us to study the interaction of pulsations and chemical peculiarities : several important astrophysical parameters such as mass, luminosity, rotational period or magnetic field strength can also be inferred, or at least constrained (Balmforth et al. 2001; Cunha 2002; Saio 2005; Bruntt et al. 2009).

However, despite several searches (e.g. Nelson & Kreidl 1993; Martínez & Kurtz 1994; Handler & Paunzen 1999; Martínez et al. 2001; Dorokhova & Dorokhov 2005; Joshi et al. 2006) only about 40 roAp stars are known to date (Kochukhov 2008a). This dearth of roAp stars demands high-precision systematic surveys. In this context, the “Nainital-Cape” survey is an effort to search pulsational variability in Ap and Am stars. In the last decade, several results were obtained from this survey. They are summarized in Table 1 : HD 12098 was discovered as a roAp star (Girish et al. 2001), and pulsations of the δ -Scuti type were discovered in 6 CP stars : HD 13038, HD 13079 (Martínez et al. 2001), HD 98851, HD 102480 (Joshi et al. 2003), HD 113878 and HD 118660 (Joshi et al. 2006).

Since the 1980’s, the high-speed photometric technique is being used to search and study the photometric light variations in short period (\sim min) pulsating variables. In parallel, high-resolution spectroscopic techniques were recently used to measure the corresponding radial velocity (RV) variations and yielded many interesting results (e.g. Kochukhov & Ryabchikova 2001; Mkrtichian et al. 2003, Hatzes & Mkrtichian 2004; Elkin et al. 2005; Kurtz et al. 2006a; Ryabchikova et al.

¹ δ -Scuti stars are pulsating variables with spectral type from A2 to F0 and luminosities ranging from zero-age main sequence to about two magnitude above the main sequence. Their known periods range from 18.12-min (HD 34282, Amado et al. 2004) to about 8-hrs, with amplitude of light variations up to a few tens of mmag. The pulsations in δ -Scuti stars are characterized by low-order, low-degree radial and/or non-radial modes which are governed by κ -mechanism operated in the He II ionization zone.

Table 1 : Pulsating variables discovered during the “Nainital-Cape survey”. HD 98851 and HD 102480 are unusual pulsators in the sense they exhibit alternating high- and low-maxima (i.e., the amplitude of the pulsations is being high and low in a cyclic way).

Star HD	P_1 (min)	P_2 (min)	Comments
12098	7.6	-	roAp type
13038	28.0	34.0	Multi-periodic δ -Scuti type
13079	73.2	-	δ -Scuti type
98851	81.0	162.0	Alternating High and Low-maxima
102480	156.0	84.0	Alternating High and Low-maxima
113878	138.6	-	δ -Scuti type
118660	60.0	151.2	Multi-periodic δ -Scuti type

2007; Kochukhov et al. 2008b; González et al. 2008). The RV measurements are a very useful technique towards the derivation of horizontal informations obtained from the line profile variability. Vertical information are extracted from the differential analysis of both amplitude and phase of spectral lines formed at different atmospheric heights. Also the phase information of individual spectral lines and oscillation modes is an important tool to constrain the chemical stratification and the physical models of the atmosphere. For these reasons, RV studies of individual lines provide a very powerful tool towards an atmospheric tomography of roAp stars.

If spectroscopic studies are such an efficient tool, why to continue doing photometric surveys ? Despite the improved sensitivity of the high-resolution spectroscopic monitoring for searching low-amplitude oscillations in roAp candidates, the major drawback of this technique remains the small amount of observing time available at large telescopes. Traditional photometric surveys are performed on small telescopes, and are consequently relatively cheap (both in cost and telescope time). For instance, Kurtz discovered the first roAp star HD 101065 by means of high-speed photometry using the 50-cm telescope of SAAO (Kurtz 1978). Indeed, this argument in favor of photometry assumes that the photometric instruments are periodically upgraded : since the 1970s, most or all bright stars that are observable with good signal to noise ratios using small telescopes and traditional detectors have been checked for pulsation at the mmag level. In order to push our investigations towards fainter objects, the technology of photometric surveys must consequently be updated with state-of-the-art instruments. This is one reason why ARIES decided to give a new impulsion to the survey by installing bigger telescopes at a better astronomical site (see Sec. 5.2, and Sagar et al. 2000; Stalin et al. 2001).

This paper is the third of a series (Paper I : Martínez et al. 2001, Paper II : Joshi et al. 2006). It is organized as follows : the selection criteria are briefly described in Sec. 2 and the technique of the observation and data analysis is described in Sec. 3. Results from the new observations of HD 25515, HD 113878 and HD 118660, along with some astrophysical parameters of these stars are presented in Sec. 4. Sec. 5 presents the null results and their analysis. Finally some conclusions are drawn in Sec. 6.

2. Selection of the Candidates

To the date, there are no firmly established selection criteria to maximize the chances of detecting new variables. Therefore our primary criterion was to choose candidates presenting Strömgren photometric indices similar to those Ap and Am stars which exhibit pulsational variability (Hauck & Mermilliod

1998). For this, the following range of Strömgren photometric indices was used to select the samples: $0.46 \leq c_1 \leq 0.88$; $0.19 \leq m_1 \leq 0.33$; $2.69 \leq \beta \leq 2.88$; $0.08 \leq b - y \leq 0.31$; $-0.12 \leq \delta m_1 \leq 0.02$ and $\delta c_1 \leq 0.04$, where c_1 is the Balmer discontinuity parameter (luminosity indicator), m_1 is the line-blanketing parameter (metallicity indicator), β is the H_β line strength index (indicator of temperature in the spectral range A3 to F2 and reasonably free from reddening), and $b - y$ is also an indicator of temperature, affected by reddening. A more negative value of δm_1 [m_1 (standard)- m_1 (observed)] and δc_1 [c_1 (observed)- c_1 (standard)] means that the star is more peculiar (Crawford 1975, 1979). However, we have slightly extended (by $\approx 10\%$) the corresponding range of indices to include the evolved and cooler stars, hence there are sample stars not falling in the range of Strömgren photometric indices mentioned above. The candidates were also selected from the general catalogue of Ap and Am stars (Renson et al. 1991) and the fifth Michigan catalogue (Houk & Swift 1999). The roAp stars are magnetic and of the SrCrEu type, and pulsating Am stars are non-magnetic. Since both belong to the spectral class of late A to early F, samples were also selected from the Kudryavtsev et al. (2006); Bychkov et al. (2003) and Høg et al. (2000).

3. Observations and Data Analysis

The time-series photometric data consist of continuous 10-sec integrations obtained through a Johnson B -filter. An aperture of $30''$ was used to minimize flux variations caused by seeing fluctuations and guiding errors. The data reduction process comprises of visual inspection of the light curve to identify and remove the bad data points, correction for coincident counting losses, subtraction of the interpolated sky background and correction for the mean atmospheric extinction. After applying these corrections, the times of the mid-points of each data samples are converted into Heliocentric Julian dates (HJD) with an accuracy of 10^{-5} day (≈ 1 s). The reduced data comprise a time-series of HJD and B-magnitude with respect to the mean of the light curve.

To search periodic signals, the time-series data were classically analyzed using a fast algorithm based on Deeming's Discrete Fourier Transform (DFT) for unequally spaced data (Deeming 1975). The first step of the analysis is to inspect the DFTs of each individual light curve where the dominant frequency f_1 is identified. To identify other frequencies present in the data, a sinusoid corresponding to the dominant frequency, amplitude and phase (of the form $A_1 \cos(2\pi f_1 t + \phi_1)$) is subtracted from the time-series. The residuals of this fit are then used to compute the DFT again, the resulting dominant frequency is identified as f_2 and so on. This prewhitening procedure was repeated until the residuals were judged to be at the noise level. To search additional frequencies and to define the known frequencies in a better way, we also computed the DFTs of the combined data sets for each star. We comment further on the data analysis in the next section.

4. New Observations of HD 25515, HD 113878 and HD 118660

The following subsections describe the results from the follow-up observations and discuss some of the fundamental astrophysical parameters of the individual stars.

Table 2 : Journal of observations of HD 25515. A value x in the Start Time HJD columns means Heliocentric Julian Date $2450000+x$. The data sets marked with asterisks are used for frequency analysis to search for the additional frequencies and define the known frequencies in a better way.

S. No.	UT Date	Start time HJD	Δt (hr)	f_1, f_2 (mHz)	A_1, A_2 (mmag)
1.	06-01-04	3011.14446	1.54	0.12 ± 0.08 0.14 ± 0.08	21.10 5.00
2.	07-01-04	3012.14302*	3.94	0.11 ± 0.04 0.19 ± 0.05	32.68 4.15
3.	11-01-04	3016.13736*	3.96	0.10 ± 0.03 0.18 ± 0.02	17.39 2.51
4.	12-01-04	3017.18221	2.21	0.13 ± 0.07 0.21 ± 0.05	28.78 9.76
5.	05-02-04	3041.08654*	2.47	0.11 ± 0.07 0.16 ± 0.09	15.07 2.29
6.	10-02-04	3046.07930*	1.92	0.12 ± 0.07 0.27 ± 0.08	15.91 4.70
7.	16-10-05	3660.27181	5.07	0.10 ± 0.03 0.14 ± 0.03	29.76 10.16
8.	17-11-05	3661.32755	3.86	0.11 ± 0.03 0.04 ± 0.03	31.51 12.92
9.	12-11-05	3687.23566*	5.40	0.10 ± 0.03 0.03 ± 0.02	35.99 11.29
10.	13-11-05	3688.30109	4.24	0.04 ± 0.03 0.06 ± 0.03	46.88 13.37
11.	14-11-05	3689.14266*	5.48	0.03 ± 0.02 0.12 ± 0.03	78.01 25.03
12.	20-12-07	4455.06725	6.59	0.10 ± 0.02 0.03 ± 0.02	33.73 9.33
13.	12-12-08	4813.14728*	5.36	0.03 ± 0.02 0.10 ± 0.03	69.02 39.10
Σ			57.52		

4.1. HD 25515

The Strömgren indices of HD 25515 are $b - y = 0.262$, $m_1 = 0.177$, $c_1 = 0.745$ and $H_\beta = 2.706$ (Hauck & Mermilliod 1998). On the basis of these peculiar indices, HD 25515 was included in the survey programme. Chaubey & Kumar (2005) announced the discovery of a pulsational period of 2.8-hrs in HD 25515, but so far no light curves had been published in the literature. Since year 2004, a total of 57.52-hrs data was collected on 13 nights. The left panel of Fig. 1 shows four typical light curves of HD 25515 and the corresponding amplitude spectra of these light curves are shown in the right panel. Table 2 gives the complete journal of the photometric observations. Columns 5 and 6 of this table list the prominent frequencies and the corresponding amplitudes, respectively. A frequency analysis of the longest time-series (Dec. 20, 2007) evidences a pulsational period of 2.78-hrs ($f_1 = 0.10 \pm 0.02$ -mHz). Another prominent frequency $f_2 \approx 0.03$ -mHz is also visible in some amplitude spectra; however, it lies in the region where the sky transparency has a high power, further follow-up observations are therefore needed to claim the detection of this frequency.

4.2. HD 113878

HD 113878 was discovered as a δ -Scuti type pulsator by Joshi et al. (2006). To confirm the pulsational variability and search for additional periodicities, follow-up observations of HD 113878 were carried out. A total of 35.97-hrs photometric data was obtained on 11 nights between year 2002 and 2008. The left panel of Fig. 2 shows the light curves of HD 113878 obtained on four observing seasons and the corresponding amplitude spectra are shown in the right panel. Table 3 lists the complete journal of these observations. Columns 5 and 6 of this table list the prominent frequencies and the corresponding amplitudes. The fre-

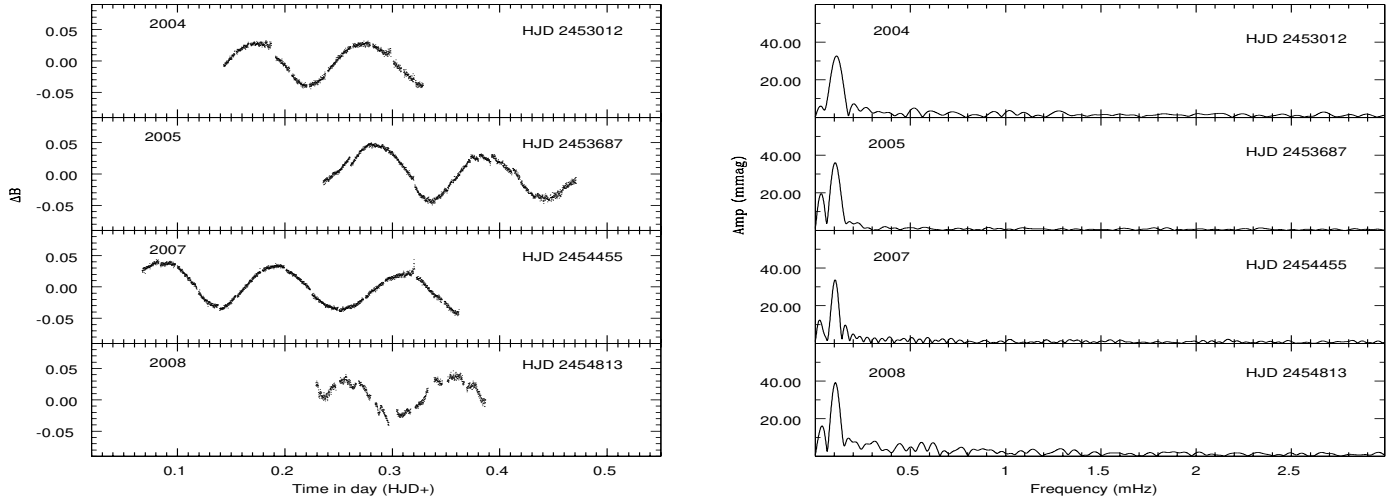


Fig. 1 : Four typical light curves (left) and their corresponding amplitude spectra (right) of HD 25515 obtained on four different observing seasons.

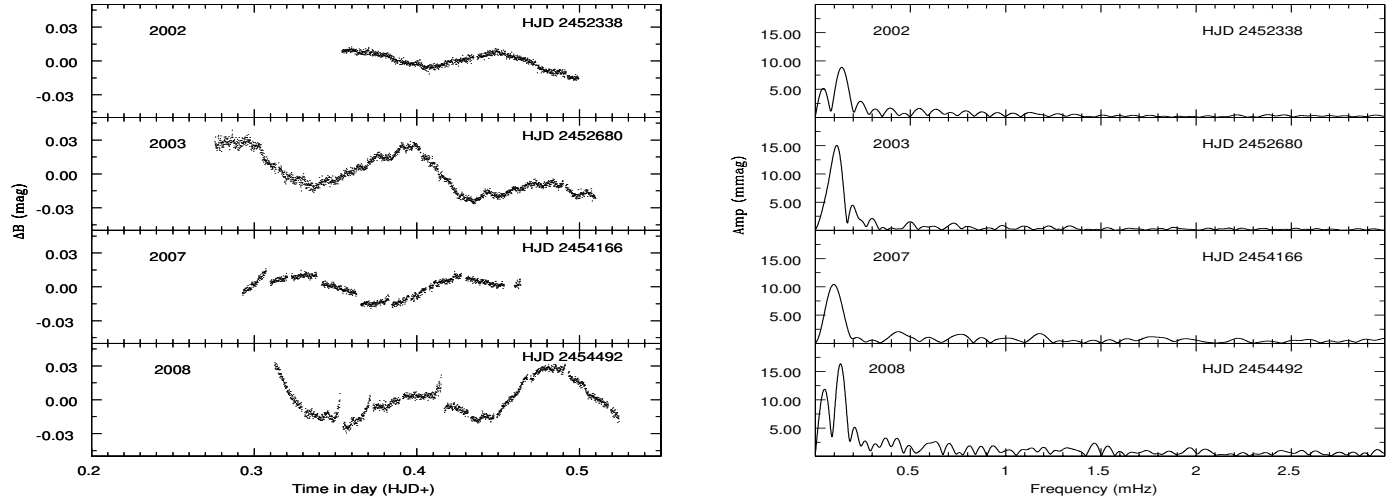


Fig. 2 : Four typical curves (left) and corresponding amplitude spectra (right) of HD 113878 obtained on four different observing seasons.

quency $f_1=0.12$ -mHz reported by Joshi et al. (2006) appears as the prominent peak in almost all the observing runs. Therefore, these 36-hrs of photometric observations confirm the period of pulsations in HD 113878. Based on the available data, presently nothing can be said about other possible frequencies.

4.3. HD 118660

The discovery of pulsations in HD 118660 was also reported by Joshi et al. (2006); it was speculated that the star might be a multi-periodic pulsating variable. To confirm this periodicity and search for additional periods, follow-up observations were carried out between year 2005 and 2007. A total of 41.22-hrs high-speed photometric data was acquired on 11 nights. Table 4 gives the journal of the observations. The left panel of Fig. 3 shows two typical light curves obtained on two observing seasons and the corresponding amplitude spectra are shown in the right panel. The frequencies $f_1=0.28$ -mHz and $f_2=0.11$ -mHz reported by Joshi et al. (2006) are indeed present in almost all the

runs, so these new observations confirm the previously known frequencies.

4.4. Frequency Analysis of the Combined Data

We combined the time-series data sets of HD 25515, HD 113878 and HD 118660 (Table 2, 3 and 4) to identify the known frequencies and to search additional frequencies. In order to obtain a good S/N ratio in the amplitude spectra, we excluded the data sets which are contaminated by large sky transparency variation and/or have duration less than one cycle. The amplitude spectra of the combined data set of HD 25515, HD 113878 and HD 118660 are shown in Fig. 4, 5 and 6, respectively. All these Fourier transforms are “raw” transforms in the sense that no low-frequency filtering to remove sky transparency fluctuations was applied to the data, other than a correction for mean extinction. The top panel of these figures are the FTs of the whole data sets mentioned in the caption of each figure while the lower panels are the FTs after successive prewhitening by f_1 ,

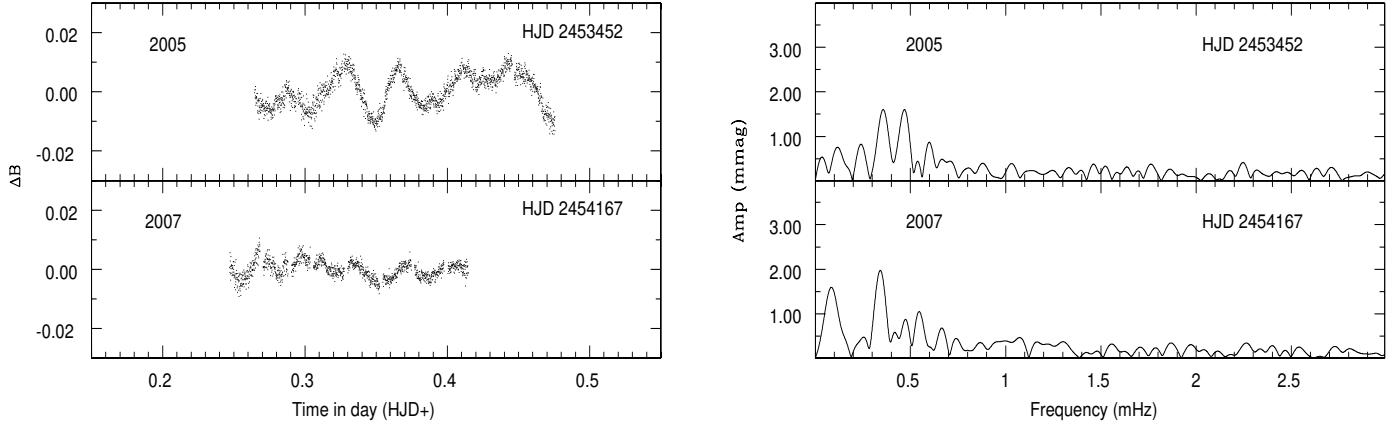


Fig. 3 : Two typical curves (left) and corresponding amplitude spectra (right) of star HD 118660 obtained on two different seasons.

Table 3 : Journal of observations of HD 113878. A value x in the Start Time HJD columns means Heliocentric Julian Date $2450000+x$. The data sets marked with asterisks are used for frequency analysis to search for the additional frequencies and define the known frequencies in a better way.

S. No.	UT Date	Start time HJD	Δt (hr)	f_1, f_2 (mHz)	A_1, A_2 mmag
1.	20-01-02	2295.52971	0.66	0.29 ± 0.20 0.26 ± 0.16	5.97 3.03
2.	14-02-02	2320.40533*	1.49	0.13 ± 0.05 0.13 ± 0.04	10.31 2.38
3.	27-02-02	2333.45894	1.09	0.16 ± 0.06 0.26 ± 0.06	11.90 3.03
4.	04-03-02	2338.35401*	3.36	0.13 ± 0.05 0.06 ± 0.04	8.87 3.17
5.	10-01-03	2650.42210*	2.22	0.11 ± 0.08 0.24 ± 0.05	10.45 0.91
6.	12-01-03	2652.35300*	3.66	0.11 ± 0.04 0.15 ± 0.07	6.63 1.00
7.	24-01-03	2664.32537	3.93	0.08 ± 0.05 0.16 ± 0.08	5.10 1.94
8.	09-02-03	2680.27589	5.38	0.03 ± 0.02 0.11 ± 0.04	15.97 15.02
9.	06-03-07	4166.29280	3.52	0.09 ± 0.04 0.15 ± 0.08	10.42 2.88
10.	26-01-08	4492.31272	4.68	0.03 ± 0.02 0.13 ± 0.03	49.10 16.38
11.	18-03-08	4544.16985	5.98	0.04 ± 0.02 0.12 ± 0.10	86.61 26.01
Σ			35.97		

f_2, f_3 , etc. Column 2, 3 and 4 of Table 5 lists the prominent frequencies, amplitudes and phases. Two frequencies $f_1=0.11$ -mHz and $f_2=0.03$ -mHz are clearly visible in the amplitude spectrum of HD 25515. However, the frequency f_2 lies in the region of sky transparency variations and hence needs confirmation. In the case of HD 113878, the frequency f_1 is present in both the combined and individual data sets and hence this frequency is firmly confirmed. The amplitude spectrum of HD 118660 clearly shows the presence of three prominent peaks at frequencies $f_1=0.054$, $f_2=0.299$ and $f_3=0.200$ -mHz. The frequency f_1 has a low amplitude and a low frequency so it should be taken cautiously.

The frequencies identified using the DFT were fitted simultaneously to the combined data by linear least-squares, which assumes that the frequencies are perfectly known and adjusts the amplitudes and phases. These amplitudes and phases, along with their errors, are listed in Table 5. The comparison of the amplitude and phase determined using both methods are consistent to

Table 4 : Journal of observations of HD 118660. A value x in the Start Time HJD columns means Heliocentric Julian Date $2450000+x$. The data sets marked with asterisks are used for frequency analysis to search for the additional frequencies and define the known frequencies in a better way.

S. No.	UT Date	Start time HJD	Δt (hr)	f_1, f_2, f_3 (mHz)	A_1, A_2, A_3 (mmag)
1.	24-02-05	3426.38106*	2.98	0.06 ± 0.05 0.10 ± 0.07 0.28 ± 0.05	19.98 7.02 5.80
2.	22-03-05	3452.26468*	4.92	0.28 ± 0.04 0.11 ± 0.03 0.04 ± 0.04	5.08 3.85 2.55
3.	28-03-05	3458.26445	5.08	0.04 ± 0.03 0.09 ± 0.05 0.05 ± 0.03	51.21 16.56 15.15
4.	29-03-05	3459.21991	1.63	0.12 ± 0.04 0.23 ± 0.08 0.48 ± 0.06	27.85 15.73 6.21
5.	30-03-05	3460.27455	4.54	0.03 ± 0.03 0.05 ± 0.03 0.10 ± 0.03	110.51 40.86 25.04
6.	31-03-05	3461.27213	5.03	0.03 ± 0.02 0.06 ± 0.03 0.10 ± 0.03	73.51 30.92 14.08
7.	04-04-05	3465.22807	3.86	0.05 ± 0.04 0.08 ± 0.03 0.13 ± 0.03	31.01 10.85 8.25
8.	05-01-07	4106.39305*	2.59	0.07 ± 0.05 0.31 ± 0.06 0.13 ± 0.05	6.62 4.25 1.49
9.	04-03-07	4164.25019*	3.52	0.25 ± 0.08 0.33 ± 0.04 0.10 ± 0.05	3.96 3.02 1.24
10.	05-03-07	4165.33844*	2.51	0.06 ± 0.05 0.28 ± 0.07 0.08 ± 0.06	6.06 2.69 1.49
11.	07-03-07	4167.24710	4.56	0.04 ± 0.03 0.04 ± 0.04 0.27 ± 0.02	19.64 4.22 3.76
Σ			41.22		

each other. We caution that all the frequencies listed in Table 5 are subject to 1-day^{-1} cycle count ambiguities. In order to reduce these ambiguities and eliminate them altogether a multi-site campaign is necessary. Note that another efficient way to study the pulsational variability in δ -Scuti type variables is the differential CCD photometry. This technique needs nearby comparison stars of similar magnitude and color. HD 25515, HD 113878 and HD 118660 are however brighter than nine magnitude and there are no nearby comparison stars of similar magnitude and

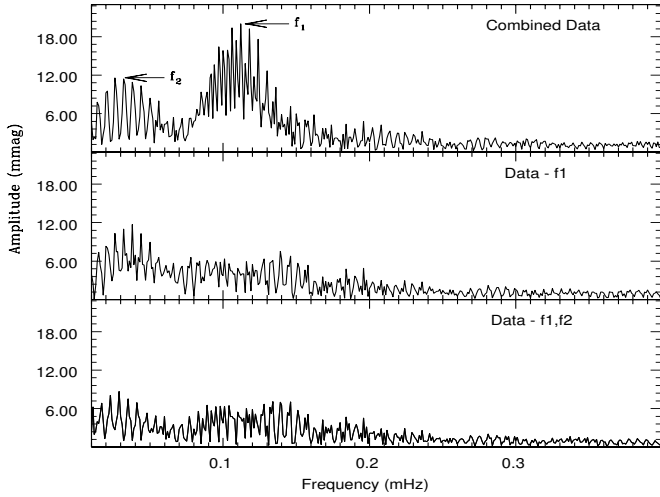


Fig. 4 : Amplitude spectrum of HD 25515 after combining the time-series data marked with asterisks in Table 2.

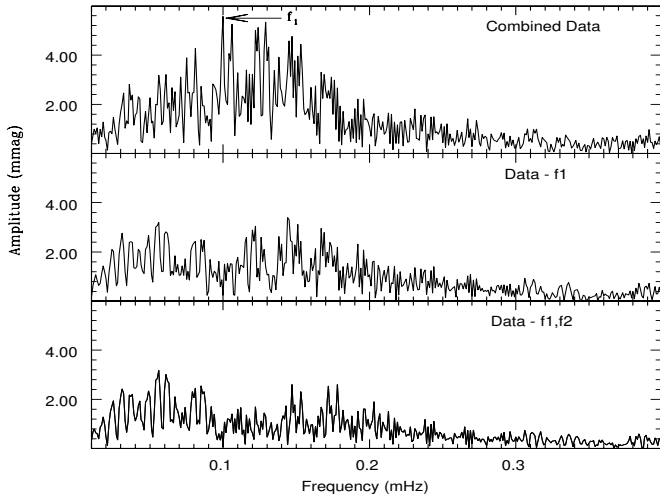


Fig. 5 : Amplitude spectrum of HD 113878 after combining the time-series data marked with asterisks in Table 3.

color; this renders the use of differential photometry difficult in this case.

4.5. Fundamental Parameters

We derived some astrophysical parameters of HD 25515, HD 113878 and HD 118660 using *Hipparcos* parallaxes (van Leeuwen 2007) and *Simbad* data. Those are listed in Table 6. The calculated values for $E(B-V)$ and the bolometric corrections (BC) for HD 25515, HD 113878 and HD 118660 are 0.02, 0.20, 0.06-mag and 0.026, 0.035, 0.035-mag, respectively. The effective temperatures of these stars were estimated using the grids of Moon & Dworetzky (1985) with typical errors of the

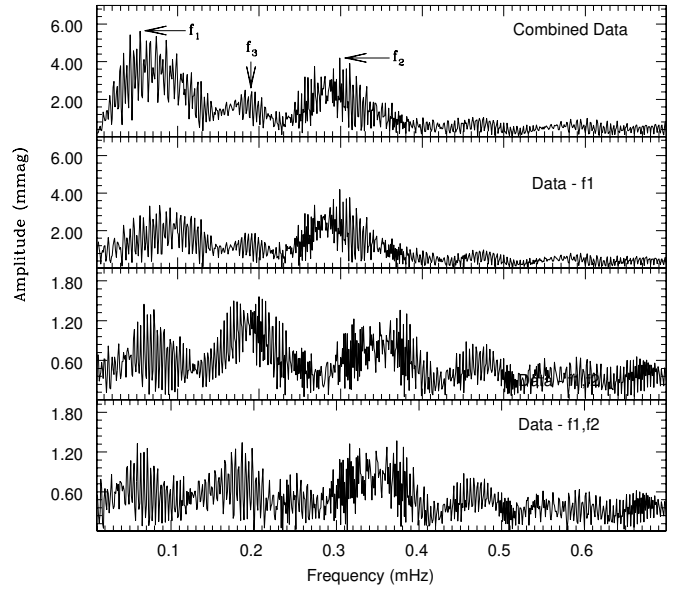


Fig. 6 : Amplitude spectrum of HD 118660 after combining the time-series data marked with asterisks in Table 4.

Table 5 : Identification of the frequencies present in HD 25515, HD 113878 and HD 118660 after combining the time-series data sets marked with asterisks in Table 2, 3 and 4, respectively. The phase ϕ corresponds to $t_0=24553012.14302$, 2452320.40523 and 2453426.38106 for HD 25515, HD 113878, and HD 118660, respectively.

Star	HD	DFT		LST	
		f	A ϕ	A ϕ	
25515	0.112	20.01	-1.482	22.40 ± 0.33	-1.513 ± 0.015
	0.038	11.68	2.964	9.53 ± 0.33	-3.020 ± 0.036
113878	0.100	5.57	0.227	5.60 ± 0.13	0.279 ± 0.023
118660	0.054	5.62	2.485	5.90 ± 0.17	2.563 ± 0.028
	0.299	4.18	-1.732	4.23 ± 0.17	-1.766 ± 0.039
	0.200	1.56	-0.815	1.77 ± 0.17	-0.684 ± 0.094

order of 200 K .

The absolute magnitude M_V is calculated using the relation (Cox 1999)

$$M_V = m_V + 5 + 5 \log \pi - A_V, \quad (1)$$

where π is trigonometric parallax measured in arcsec, the interstellar extinction in the V-band is $A_V = R_V E(B-V) = 3.1 E(B-V)$. The reddening parameter $E(B-V)$ is obtained by taking the difference of observed color (taken from *Simbad* data sets) and intrinsic color (estimated from Cox 1999).

Table 6 : Astrophysical data for HD 25515, HD 113878 and HD 118660 taken from Simbad Data Base , Hipparcos and using the standard relations.

Star HD	m_v (mag)	π (mas)	d (pc)	M_v (mag)	T_{eff} (K)	$\log(\frac{L_*}{L_\odot})$
25515	8.70	5.41±0.91	185±32	2.30±0.84	6823	0.97±0.34
113878	8.24	2.49±0.77	402±137	-0.40±1.55	7263	2.04±0.62
118660	6.50	13.65±0.36	73±2	2.12±0.14	7500	1.03±0.05

The luminosity $\log(\frac{L_*}{L_\odot})$ were calculated using the relation

$$\log\left(\frac{L_*}{L_\odot}\right) = -\frac{M_v + BC - M_{bol,\odot}}{2.5}, \quad (2)$$

where $M_{bol,\odot} = 4.74$ (Cox 1999), and the bolometric correction BC is estimated using the interpolation from Flower (1996).

The estimated positions of HD 25515, HD 113878 and HD 118660 in the H-R diagram are shown in Fig. 7. For comparison, evolutionary tracks² of mass ranging from 1.6 to 2.9 M_\odot are also over-plotted (Christensen-Dalsgaard 1993). These models are computed with the Aarhus evolution code (ASTEC), superior in terms of numerical precision and used extensively (Cunha 2002, Freyhammer et al. 2008a, 2008b). For the model calculations, we used the compositions $X = 0.692827$ and $Z = 0.02$, the equation of state from Eggleton et al. (1973), opacities from OPAL92, and the convection was treated with mixing-length theory. No convective-core overshoot, diffusion and settling was considered to compute these models (J. Christensen-Dalsgaard, personal communication). The position of the blue (left) and red edge (right) of the instability strip are shown by two straight lines (Turcotte et al. 2000). The error in the determination of the luminosity of HD 113878 is quite significant due to large uncertainty in the parallaxes. From this figure it is clear that the mass of these stars are well within the range of δ -Scuti stars. The H-R diagram also suggests that HD 25515 and HD 118660 are in the Hydrogen burning phase while HD 113878 is in the Helium burning phase.

5. Null Results

The candidate stars for which no pulsational variability could be ascertained are addressed as null results. The null results are either constant stars, or pulsating variables with amplitude of variations below the detection limit. Consequently, the frequency spectra of the light curves of such candidates do not show any peak to be considered as the signature of pulsations.

It should be kept in mind that the rotational amplitude modulation and beating between frequencies may result in pulsations not being visible during particular observations (Martinez & Kurtz 1994, Handler 2004). So if a star is classified as a null result in a particular observation, it does not mean that the star is non-variable. For example, HD 25515 (Sec. 4.1) was observed for a duration of 0.78-hr on HJD2451832 and did not show any pulsational variability; it was hence classified a null result (Joshi et al. 2006) although it is a variable.

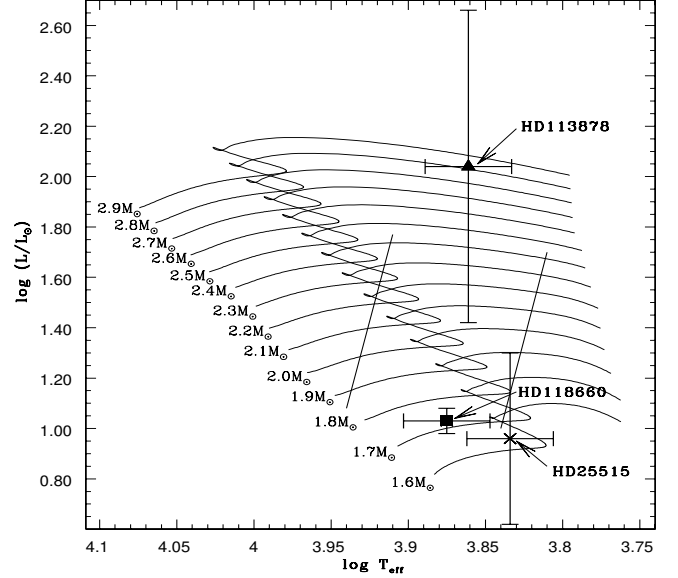


Fig. 7 : An HR diagram showing the positions of HD 25515 (cross), HD 113878 (triangle) and HD 118660 (square) in relation to the borders of the instability strip. For the comparison evolutionary tracks of 1.6 to 2.9 M_\odot stars are over-plotted.

The null results are therefore important for comparison with further studies. In addition, the null result light curves are considered as essentially composed from noise, so they reflect the quality of the observation conditions. The database composed by the null results light curves is therefore very interesting for statistical studies of all noise sources (instruments, atmosphere etc.) active during the observations.

5.1. Fundamental Astrophysical Parameters

Since the last survey paper (Joshi et al. 2006) a total of 61 candidate stars were monitored to search for pulsational variability (in addition to the 3 variables described above) and few of them were observed several times. Table 7 (only available in electronic form) lists the different astrophysical parameters of the studied sample, either available in the Simbad data base or calculated using the standard relations. For each stars, the columns of this table list respectively the HD number, right ascension α_{2000} , declination δ_{2000} , visual magnitude m_v , spectral type, parallax π (van Leeuwen 2007), spectral indices $b - y$, m_1 , c_1 , H_β , δm_1 , δc_1 , effective temperature T_{eff} , reddening parameter $E(B-V)$, absolute magnitude M_v , luminosity $\log(\frac{L_*}{L_\odot})$ (Sec. 4.5), duration of the observations Δt , Heliocentric Julian Dates (HJD) and year of observations when the star was observed. Visual magnitude m_v , spectral type, parallax π , spectral indices $b - y$, m_1 , c_1 and H_β are taken from the Simbad data base. δm_1 and δc_1 are calculated using the calibration of Crawford (1975,1979) and T_{eff} is calculated using the grids of Moon & Dworetzky (1985). The typical error in the estimation of the effective temperature of sample stars is about 200 K.

Fig. 11 (only available in electronic form) shows the amplitude spectra of the light curves corrected for extinction. As we are searching pulsational variability of the mmag order in the period range of a few minutes to a few hours, an amplitude

² http://www.phys.au.dk/jcd/emdl94/eff_v6

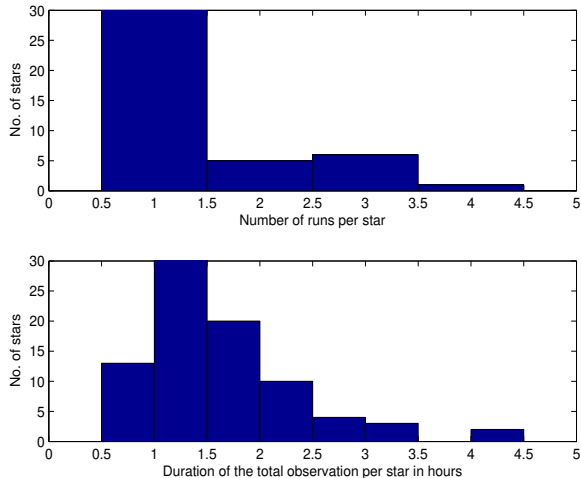


Fig. 8 : Statistics of the 87 runs acquired by the Nainital-Cape survey in the time range 2002-2008. Top: Distribution of the number of runs per star. Most of the stars have been observed only once. A few of them, where some variability was suspected, were observed many times. Bottom: Distribution of the total time dedicated to observe one star (in hours). Most of the stars have been observed less than 2-hrs (the mean is 1.6-hrs and the median 1.5-hrs).

scale of 0 to 9 mmag in the y-axis and frequency scale of 0 to 5-mHz in x-axis are chosen. The data reduction process is common for all stars so their spectra form a relatively homogeneous set of data. Fig. 12 (only available in electronic form) shows the prewhitened spectra that have been filtered for low-frequency sky transparency variations. The prewhitening strategy was to remove the high energy (above 3 mmag) low-frequency peaks (below ≈ 0.5 -mHz).

5.2. Analysis of the Null Results

Before proceeding further, we have to correct for two informations regarding the null results presented in the previous survey paper (Joshi et al. 2006). Firstly, the time span of the data set in the previous paper was not 1999-2004, as mentioned in the text, but 1999-2002 (precisely 1999 November 15, to 2002 March 05). Secondly, Fig. 7 and 8 were interchanged. These figures are very similar to each other so it does not change the essence of the comments, but we nevertheless apologize to the readers and to the Editor.

Fig. 8 shows the distribution of the number of runs per star, and the duration of the runs per star for the 2002-2008 data. These plots show the detection strategy of the observations : observe the candidates for a short time in order to check several targets per night.

Fig. 9 shows the amplitude distribution of the tallest peak in the prewhitened spectra presented in the end of the paper. While in 2-hrs the level of the maxima of the noise peak created by scintillation is about 0.2-mmag for best photometric nights (Mary 2006), it has higher values for many nights. This is mainly because of powerful low frequency noise (sky transparency variation), that is not totally removed by prewhitening. Most light curves have their highest peak around 0.3 to 1-mmag. This range can be considered as an operational detection limit. Notice that for quite a few nights, the highest peak has a much higher ampli-

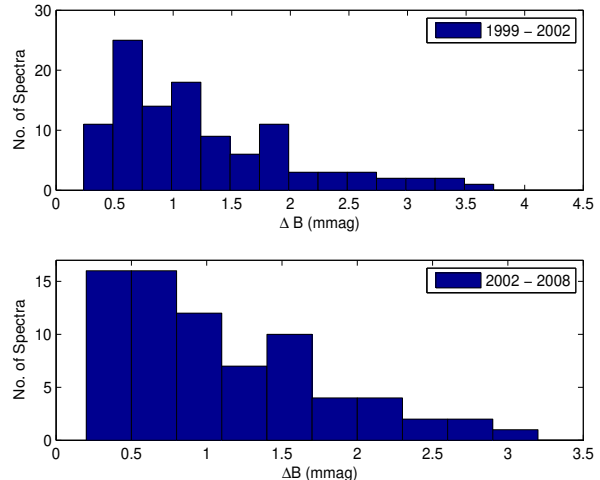


Fig. 9 : Distribution of the amplitude of the tallest peaks in the prewhitened spectra for the 1999-2002 data (top) and 2002-2008 data (bottom).

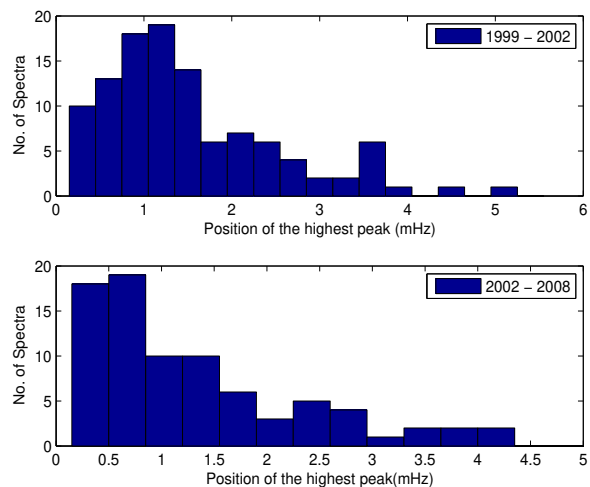


Fig. 10 : Distribution of the positions of the tallest peaks in the prewhitened spectra for the 1999-2002 data (top) and 2002-2008 data (bottom).

tude. The mean of the distribution is 1.42 ± 0.14 -mmag and the median 1.0-mmag. For the data set of the previous observation period (Nov. 99 to March 2002), we had for the amplitude distribution of the highest peak a mean of 1.25 ± 0.07 -mmag and a median of 1.0-mmag. While the median is stable, the mean indicates a slight increase in the average power of the noise during the last 6 years with respect to the time period 1999-2002.

Fig. 10 shows the distribution in position (mHz) of the highest peak. The distribution is not flat as would be expected from a purely scintillation noise spectrum; this is again due to sky transparency variations. The mean and the median are respectively 1.25 ± 0.11 -mHz and 0.9-mHz, against 1.52 ± 0.10 -mHz and 1.3-mHz for the 1999-2002 data set. This indicates that the highest peak is shifted to the low frequency part of the spectrum, suggesting in turn that sky transparency variations (occurring at lower frequencies) are getting more powerful as before.

Astronomers used to the Nainital site have observed a slight decrease in the photometric quality of Manora Peak's sky (where ARIES is located), mainly because of an increase of the human activity in the surroundings. ARIES is now in the process of installing 1.3-m and 3.6-m optical telescopes at a new astronomical site, Devasthal (longitude: 79°40'57" East, latitude : 29°22'26" North, altitude : 2420-m) by the end of year 2009 and 2012, respectively. This site has an average seeing of $\approx 1''$ near ground and $\approx 0.65''$ at 12-m above the ground (Sagar et al. 2000; Stalin et al. 2001). We expect these new observing facilities at Devasthal to contribute significantly to the area of asteroseismology in a very near future.

6. Conclusions

On the basis of about 58-hrs high-speed photometric data acquired on 13 nights on different observing seasons, it is found that HD 25515 pulsates with a period of about 2.78-hrs. HD 113878 was observed for 36-hrs on 11 nights during different seasons and no new frequency could be detected because the data are severely aliased. However, the previously estimated frequency (0.12-mHz) is present in all data sets. Similarly, in the 41-hrs time-series photometric observations of HD 118660 taken on 11 nights, we could not identify any new frequencies other than the previously known. The fundamental astrophysical parameters of these stars were calculated using standard relations and summarized in Table 6. The positions of HD 25515, HD 113878 and HD 118660 in the H-R diagram indicate that all these stars are near the red-edge of the instability strip, where most pulsating variables are found in general. The H-R diagram also shows that HD 25515 and HD 118660 are near the MS, while HD 113878 is an evolved star. We have also presented a catalogue of 61 null results stars acquired over the time scale 2002-2009, along with 87 spectra. A statistical analysis of these null results shows, by comparison with past data, that the photometric quality of the nights at ARIES has slightly decreased during the last few years. The Nainital-Cape survey is an ongoing project, and in the light of the up-coming observational facilities, the future of asteroseismology at ARIES is quite promising.

7. Acknowledgments

We are thankful to the anonymous referee for many useful comments which helped us improving substantially the manuscript. The authors acknowledge Prof. R. Sagar, Prof. D. W. Kurtz, Drs. P. Martinez, S. Seetha, B. N. Ashoka, U. S. Chaubey and V. Girish for their participation in the "Nainital-Cape-Survey". SKT is thankful to Prof. U. S. Pandey for his critical reading. Resources provided by the electronic databases (SIMBAD, NASA's ADS and Hipparcos) are acknowledged. This work was carried out under the Indo-South Africa Science and Technology Cooperation (INT/SAFR/P-04/2002/13-02-2003 and INT/SAFR/P-3(3)2009).

References

- Amado, P. et al., 2004, in *The A-Star Puzzle*, eds. J. Zverko, W. W. Weiss, J. Žižňovský, S. J. Adelman, W. W. Weiss, Cambridge University Press, IAUS, 224, 863
- Balmforth, N. J., Cunha, M. S., Dolez, N., Gough D. O., & Vauclair, S., 2001, *MNRAS*, 323, 362
- Bigot, L. & Dziembowski, W. A., 2002, *A&A* 391, 235
- Breger, M., 1970, *ApJ*, 162, 597
- Bruntt, H. et al., 2009, *MNRAS*, 396, 1189
- Bychkov, V. D., Bychkova, L. V. & Madej, J., 2003, 407, 631
- Carrier, F., Eggenberger, P., Leyder, J.-C., Debernardi, Y., Royer, F., 2007, *A&A*, 470, 1009
- Chaubey, U. S. & Kumar, N. S., 2005, *BASI*, 33, 371
- Christensen-Dalsgaard, J., 1993, in *Inside the stars*, Baglin A., Weiss W. W., eds, *ASP Conf. Ser. Vol. 40, Proc. IAU Coll. 137*, ASP, 483
- Cox, N., *Allen's Astrophysical Quantities*, 1999
- Crawford, D. L., 1975, *AJ*, 80, 955
- Crawford, D. L., 1979, *AJ*, 84, 1858
- Cunha, M. S., 2002, *MNRAS*, 333, 47
- Deeming, T. J., 1975, *Ap&SS*, 36, 137
- Dorokhova, T. & Dorokhov, N., 2005, *JApA*, 26, 223
- Eggleton, P. P., Faulkner, J., Flannery, B. P., 1973, *A&A*, 23, 325
- Elkin, V. G., Riley, J. D., Cunha, M. S., et al., 2005, *MNRAS*, 358, 665
- Freyhammer, L. M., Elkin, V. G., Kurtz, D. W., 2008a, *MNRAS*, 390, 257
- Freyhammer, L. M., Kurtz, D. W. et al., 2008b, *MNRAS*, 385, 1402
- Flower, B. J., 1996, *ApJ*, 469, 355
- Girish, V., Seetha, S., Martinez, P., Joshi, S., et al., 2001, *A&A*, 380, 142
- González, J. F., Hubrig, S., Kurtz, D. W., Elkin, V., Savanov, I., 2008, *MNRAS*, 384, 1140
- Handler, G. & Paunzen, E., 1999, *A&AS*, 135, 57
- Handler, G., 2004, *Communication in Asteroseismology*, 145, 71
- Hatzes, A. P. & Mkrtychian, D. E., 2004, *MNRAS*, 351, 2
- Hauk, B. & Mermilliod M., 1998, *A&AS*, 129, 431
- Hekker, S., Fremat, Y., Lampens, P., De Cat, P., 2008, 157, 317
- Gregory, H. W., Francis, F. C., 2005, *AJ*, 129, 202
- Høg, E., Fabricius, C., Makarov V. V. et al., 2000, *A&A*, 355, L27
- Houk, Nancy & Swift, Carrie, 1999, *Michigan catalogue of two-dimensional spectral types for the HD Stars ; vol. 5*
- Joshi, S., Girish, V., Sagar, R., Kurtz, D. W., et al., 2003, *MNRAS*, 344, 431
- Joshi, S., Mary, D. L., Martinez, P., Kurtz, D. W., et al., 2006, *A&A*, 455, 303
- King, H., Matthews, J. M. et al. 2007, *Comm. in Asteroseismology*, 2006, 148, 28
- Kochukhov, O. & Ryabchikova, T., 2001, *A&A*, 374, 615
- Kochukhov, O., Bagnulo, S., Wade, G. A. et al., 2004a, *A&A*, 414, 613
- Kochukhov, O., Drake, N. A. et al., 2004b, *A&A*, 424, 935
- Kochukhov, O. & Bagnulo, S., 2006, *A&A*, 450, 763
- Kochukhov, O., In the *Proceedings of the Wrocław HELAS, Workshop 2008*, M. Breger, W. Dziembowski M. Thompson eds., *Communications in Asteroseismology*, 2008a, 157,
- Kochukhov, O., Ryabchikova, T., Bagnulo, S., LoCurto, G., 2008b, *A&A*, 479, L29
- Kreidl, Tobias J., 1985, *IBVS*, 2739
- Kudryavtsev, D. O., Romanyuk, I. I., Elkin, V. G., Paunzen, E., 2006, *MNRAS*, 372, 1804.
- Kurtz, D. W., 1978, *IBVS*, 1436, 1
- Kurtz, D. W., 1982, *MNRAS*, 200, 807
- Kurtz, D. W., 1989, *MNRAS*, 238, 1077
- Kurtz, D. W. & Martinez P., 2000, 9, 253
- Kurtz, D. W., Cameron, C., Cunha, M. S., et al. 2005, *MNRAS*, 358, 651
- Kurtz, D. W., Elkin, V. G., Mathys, G., 2006a, *MNRAS*, 370, 1274
- Kurtz, D. W., Elkin, V. G., Cunha, M. S. et al. 2006b, *MNRAS*, 372, 286
- Leblanc, F & Alecian, G., 2008, *A&A*, 477, 243
- Leblanc, F., Monin, D. Hui-Bon-Hoa, A., Hauschildt, P. H., 2009, *A&A*, 495, 937
- Lueftinger, T., Kuschnig, R., Piskunov, N. E., Weiss, W. W., 2003, *A&A*, 406, 1033
- Michaud, G., Tarasick, D., Charland, Y., Pelletier, C., 1983, *ApJ*, 269, 239
- Mkrtychian, D. E., Hatzes, A. P., Kanaan, A., 2003, *MNRAS*, 345, 781
- Martinez, P., & Kurtz, D. W., 1994, *MNRAS*, 271, 129
- Martinez, P., Kurtz, D. W. et al., 1999, *MNRAS*, 309, 871
- Martinez, P., Kurtz, D. W., Ashoka, B. N., Chaubey, U. S., Girish, V., Joshi, S., et al. 2001, *A&A*, 371, 1048
- Mary, D. L., 2006, *A&A*, 452, 715
- Michaud, G. 1970, *ApJ*, 160, 641
- Michaud, G., Charland, Y., Megessier, C. 1981, *A&A*, 103, 244
- Moon, T. & Dworetzky, M. M., 1985, *MNRAS*, 217, 305
- Nelson, M. J., & Kreidl, T. J., 1993, *AJ*, 105, 1903
- Renson P., Gerbaldi M., Catalano F. A., 1991, *A&AS*, 89, 429
- Ryabchikova, T., Piskunov, N., Kochukhov, O., et al. 2002, *A&A*, 384, 545
- Ryabchikova, T., Leone, F., Kochukhov, O. 2005, *A&A*, 438, 973
- Ryabchikova, T., Ryabtsev, A., Kochukhov, O., Bagnulo, S. 2006, *A&A*, 456, 329
- Ryabchikova, T., Sachkov, M., Weiss, W. W. et al., 2007, *A&A*, 462, 1103
- Saio, H., 2005, *MNRAS*, 360, 1022
- Sagar, R., Stalin, C. S., Pandey, A. K., et al. 2000, *A&AS*, 144, 349
- Stalin, C. S., Sagar, R., Pant, P., et al., 2001, *BASI*, 2001, 29, 39
- Turcotte, S., Richer, J., Michaud, G., Christensen-Dalsgaard, J. 2000, *A&A*, 360, 603

van Leeuwen, F., 2007, *A&A*, 474, 653

Vauclair, S. & Thádo, S., 2004, *A&A*, 425, 179

Online Material

Table 7 : Sample of stars classified as null results. The unprewhitened and prewhitened spectra of these stars are depicted in Figure 11 and Figure 12, respectively. The columns list S. No., HD number, right ascension α_{2000} , declination δ_{2000} , visual magnitude m_v , spectral type, parallax π , spectral indices $b-y$, m_1 , c_1 , $H\beta$, δm_1 , δc_1 , effective temperature T_{eff} , reddening parameter E(B-V), absolute magnitude M_V , luminosity $\log(\frac{L_*}{L_\odot})$, duration of the observations Δt , Heliocentric Julian Dates (HJD:2450000+) and year of observation (2000+). The sign “-” is for those stars for which the basis data is not available in the archive.

S. No.	Star HD	α_{2000} hh mm ss	δ_{2000} dd mm ss	m_v mag	Sp. Type	π mas	$b-y$ mag	m_1 mag	c_1 mag	β mag	δm_1 mag	δc_1 mag	T_{eff} K	E(B-V) mag	M_V mag	$\log(\frac{L_*}{L_\odot})$	Δt hr	HJD d	Year
1.	2453	00 28 28	+32 26 16	6.91	A2p	4.51 ±0.47	0.022	0.244	0.887	2.854	-0.038	2.016	9125	0.03	0.088	1.896	1.98	2569	02
2.	2957	00 32 44	-13 29 13	8.50	Ap	3.88 ±0.84	-0.008	0.209	0.991	2.880	-0.009	0.061	8350	0.03	1.351	1.351	3.33	4759	08
3.	3321	00 36 22	+33 38 39	8.40	A3	6.34 ±0.90	-	-	-	-	-	-	-	0.22	1.728	-	2.09	4397	07
4.	5601	00 57 32	-10 28 33	7.63	A0	3.58 ±0.47	-0.056	0.219	0.782	-	-	-	-	0.00	0.461	-	2.23	4758	08
5.	6757	01 08 53	+45 12 27	7.70	A0Vp	7.71 ±1.25	-	-	-	-	-	-	-	0.42	0.833	-	1.29	4757	08
6.	8855	01 28 06	+43 52 39	8.20	A1p	1.84 ±0.68	-	-	-	-	-	-	-	0.00	-0.166	-	1.06	4815	08
7.	9147	01 30 56	+45 21 56	9.38	A0p	-	-	-	-	-	-	-	-	0.11	-	-	1.05	4758	08
8.	11362	01 52 15	+26 10 05	8.63	A5	-	0.242	0.227	0.754	2.768	-0.036	0.038	7411	0.19	-	-	0.99	2653	03
9.	11543	01 55 10	+59 30 30	8.14	Am	9.36±1.03	0.144	0.214	0.857	2.846	-0.007	-0.005	8091	0.08	2.748	0.787	1.35	3720	05
10.	12163	02 00 16	+37 38 01	8.24	F0III	-	0.204	0.198	0.666	2.748	-0.012	0.036	7261	0.04	-	-	2.88	2955	03
11.	13404	02 11 54	+36 57 58	8.75	A2	6.33±1.07	0.212	0.262	0.600	2.809	-0.058	-0.198	7913	0.30	1.827	1.154	1.59	2569	02
12.	15082	02 26 51	+37 33 02	8.30	A5	8.65±0.80	0.166	0.204	0.720	2.768	-0.013	0.004	7418	0.00	3.171	0.614	1.59	3721	05
13.	16605	02 40 59	+42 52 16	9.63	F7V	-	-0.021	0.222	0.774	2.816	-0.014	0.024	7883	0.00	-	-	0.91	4759	08
14.	18078	02 56 32	+56 10 41	8.30	A0p	0.64±0.73	0.087	0.251	1.079	2.831	-0.044	0.243	7947	0.22	-3.351	3.225	1.25	3690	05
15.	19653	03 12 46	+60 48 03	8.87	B9p	2.67±1.08	0.170	0.131	1.045	-	-	-	-	0.29	0.073	-	0.76	3719	05
16.	19712	03 10 18	-01 41 41	7.35	B9	6.91±0.59	-0.060	0.227	0.860	2.858	-0.022	-0.026	11005	0.05	1.392	1.512	1.58	4815	08
17.	21476	03 32 01	+67 35 08	7.64	F0	8.74±1.16	0.231	0.155	0.591	2.707	0.018	0.039	6929	0.01	2.304	0.963	1.09	4757	08
18.	25154	03 59 48	-00 01 13	9.88	A5	6.74±1.41	0.429	0.236	0.693	2.783	-0.039	-0.053	7591	0.39	2.814	0.757	1.23	3659	05
19.	25499	04 05 39	+53 04 28	8.05	F0	-	0.225	0.238	0.690	2.744	-0.053	0.067	7217	0.08	-	-	1.21	4397	07
20.	27404	04 20 37	+28 53 31	7.95	A0	4.40±1.15	0.183	0.114	0.788	2.787	0.085	0.034	7570	0.24	0.423	1.713	1.23	2569	02
21.	27716	04 24 00	+35 12 57	7.88	F0	8.87±0.67	0.228	0.216	0.787	2.777	-0.021	0.106	7481	0.09	2.341	0.946	2.13	2954	03
22.	32428	05 04 37	+32 19 13	6.62	A4m	10.28±1.06	0.171	0.210	0.819	2.770	-0.018	0.099	7406	0.00	1.540	1.210	1.61	2954	03
23.	32642	05 05 32	+19 48 24	6.44	A5m	7.26±0.81	0.124	0.211	1.014	2.867	-0.008	0.110	8300	0.09	0.466	1.704	1.01	4758	08
24.	35450	05 28 24	+58 40 30	8.18	A3	7.42±0.87	-	-	-	-	-	-	-	0.21	1.881	-	1.36	3721	05
25.	38817	05 50 37	+44 00 41	7.56	A2	7.27±0.76	0.066	0.217	0.942	2.860	-0.012	0.052	8209	0.11	1.527	1.277	1.74	3748	06
26.	38823	05 48 25	-00 45 34	7.32	A5	10.26±0.84	0.151	0.301	0.580	-	-	-	-	0.22	1.694	-	1.70	3749	06
27.	40759	06 00 45	-03 53 44	8.56	A0	4.63±0.92	-0.013	0.226	0.899	-	-	-	-	0.05	1.733	-	1.04	4396	07
28.	43058	06 16 21	+43 39 56	9.15	A3	-	-	-	-	-	-	-	-	0.15	-	-	1.49	4397	07
																	1.39	2563	02
																	0.73	2563	02
																	3.18	2952	03
																	4.25	2953	03
																	4.28	2976	03
																	1.63	4795	08
																	0.78	4815	08
																	1.32	4758	08
																	1.12	4795	08
																	1.82	3720	05

Table 7 : Continued

S. No.	Star HD	α_{2000} hh mm ss	δ_{2000} dd mm ss	m_v mag	Sp. Type	π mas	b-y mag	m_1 mag	c_1 mag	β mag	δm_1 mag	δc_1 mag	T_{eff} K	E(B-V) mag	M_V mag	$\log(\frac{L_*}{L_\odot})$	Δt hr	HJD d	Year
29.	43508	06 20 04	+56 55 31	8.86	F0	4.32±1.29	0.206	0.215	0.844	2.790	-0.016	0.140	7600	0.01	2.006	1.080	1.34	3690	05
30.	44738	06 23 54	+14 06 49	7.90	A2	2.68±0.93	-0.071	0.244	0.807	2.799	-0.041	0.029	7650	0.01	0.009	1.879	2.97	3718	05
31.	45784	06 30 45	+29 49 42	8.11	F2	6.28±1.01	0.206	0.234	0.745	2.771	-0.041	0.074	7438	0.00	2.255	0.980	2.98	2651	03
32.	49713	06 49 44	-01 20 23	7.32	B9p	5.01±0.70	-0.051	0.184	0.655	2.747	-	-	12719	0.26	0.013	2.064	1.61	4795	08
33.	52069	07 01 22	+34 59 52	8.79	A5	-	0.199	0.220	0.712	2.757	-0.033	0.018	7350	0.18	-	-	1.19	3397	04
34.	57558	07 23 42	+42 18 56	9.07	A5	-	0.176	0.229	0.730	2.779	-0.033	-0.008	7600	0.15	-	-	2.37	3459	04
																	2.03	3464	04
																	2.67	3465	04
35.	59622	07 31 46	+23 38 53	8.69	F0	-	0.171	0.246	0.781	2.780	-0.050	0.095	7507	0.00	-	-	1.39	2654	03
36.	64534	07 55 48	+35 58 22	9.18	F0	2.31±1.18	0.098	0.283	0.871	2.862	-0.061	0.039	8228	0.00	1.308	1.366	1.06	2662	03
37.	64561	07 54 34	+01 34 13	8.24	A3	8.02±0.93	0.169	0.278	0.732	2.783	-0.081	-0.014	7548	0.25	1.986	1.088	1.26	2649	03
38.	66350	08 03 01	-02 43 49	8.68	A0	1.73±0.92	-0.030	0.197	1.050	-	-	-	-	0.00	-0.129	-	0.85	4815	08
39.	68703	08 14 11	+17 40 33	6.47	A0	10.53±0.51	0.174	0.221	0.813	2.775	-0.027	0.083	7200	0.31	0.618	1.635	0.75	3687	05
																	1.47	3688	05
																	1.08	3718	05
40.	71973	08 36 49	+74 43 25	6.31	A2m	13.21±0.50	0.169	0.236	0.766	2.767	-0.045	0.052	7400	0.23	1.202	1.401	1.57	3721	05
41.	72943	08 36 08	+15 18 49	6.32	F0IV	12.86±0.45	0.211	0.186	0.732	2.720	-0.009	0.152	7000	0.00	2.207	1.001	1.43	3812	06
42.	73093	08 38 17	+43 10 10	9.61	A5	-	0.080	0.248	0.963	2.862	-0.043	0.069	8300	0.00	-	-	1.42	3422	04
43.	73618	08 39 56	+19 33 11	7.30	Am	3.62±1.05	0.105	0.230	0.967	2.846	-0.023	0.105	8100	0.04	-0.030	1.899	1.51	3720	05
44.	73619	08 39 58	+19 32 29	7.52	Am	3.62±1.05	0.143	0.237	0.829	2.823	-0.031	0.004	7900	0.09	0.035	1.871	0.64	3689	05
45.	73709	08 40 21	+19 41 12	7.68	F2III	4.58±0.57	0.099	0.258	0.938	2.843	-0.042	0.140	8100	0.00	1.418	1.319	1.38	3719	05
																	1.10	3748	06
46.	77314	09 01 58	+02 40 16	7.14	Ap	6.78±0.91	-	-	-	-	-	-	-	0.01	1.265	-	3.12	4549	08
																	1.49	4550	08
																	1.48	4551	08
47.	86170	09 56 45	-02 17 20	8.42	A2	3.20±0.98	0.074	0.226	0.929	-	-	-	-	0.12	0.574	-	0.91	4815	08
48.	86458	10 01 32	+68 43 05	8.05	F0	6.28±0.95	0.248	0.220	0.673	2.711	-0.046	0.111	6900	0.08	1.792	1.168	0.84	3397	04
49.	94401	10 53 52	+02 39 28	8.09	F0	6.99±0.71	0.581	0.382	0.441	2.711	-0.208	-0.121	7139	0.00	2.312	0.958	1.42	3458	04
50.	95256	11 01 06	+63 25 16	6.37	A2m	11.19±0.66	0.083	0.240	0.965	2.845	-0.033	0.105	8200	0.12	1.614	1.242	2.08	3719	05
																	1.99	3721	05
																	0.98	3812	06
51.	96003	11 04 33	+12 40 01	6.87	A3p	6.06±0.49	-0.020	0.228	0.993	2.893	-0.030	0.037	9795	0.04	0.655	1.636	0.55	3717	05
52.	96528	11 07 40	+23 19 25	6.49	A5m	12.91±0.41	0.093	0.210	0.914	2.870	-0.008	0.004	8300	0.01	2.001	1.090	1.88	3718	05
53.	110248	12 40 35	+30 22 39	7.65	Am	6.59±0.67	0.181	0.251	0.789	2.808	-0.047	-0.007	7800	0.15	1.279	1.372	1.09	3397	04
54.	112097	12 53 50	+12 25 06	6.25	A7III	16.42±0.80	0.175	0.176	0.747	2.750	0.009	0.067	7300	0.08	2.245	0.984	2.37	3812	06
55.	132739	15 00 19	+13 19 17	8.59	F0p	5.49±1.02	0.226	0.169	0.703	2.719	0.008	0.125	7000	0.03	2.195	1.006	1.30	3838	06
56.	136403	15 19 30	+32 30 54	6.33	A2m	11.50±0.35	0.135	0.209	0.845	2.817	-0.004	0.031	7800	0.17	1.122	1.435	2.08	3182	06
57.	141675	15 47 38	+55 22 36	5.88	A3m	13.55±0.32	0.136	0.248	0.866	2.823	-0.042	0.041	7900	0.15	1.078	1.453	1.58	3481	04
58.	158116	17 26 14	+29 27 20	7.68	Am	4.32±0.81	0.156	0.255	0.908	2.792	-0.054	0.144	7600	0.14	0.423	1.713	1.70	3481	04
59.	190145	19 58 59	+67 28 20	7.56	A2p	6.02±0.46	0.129	0.260	0.838	2.841	-0.052	-0.014	8100	0.21	0.807	1.564	1.00	3518	04
60.	198263	20 47 24	+48 51 08	8.16	F0	-	0.217	0.267	0.684	2.764	-0.076	0.026	7400	0.05	-	-	1.83	3541	04
61.	213143	22 29 06	+21 23 35	7.75	Fm	4.00±0.73	0.229	0.246	0.729	2.753	-0.058	0.090	7300	0.07	0.543	1.665	1.66	3690	05

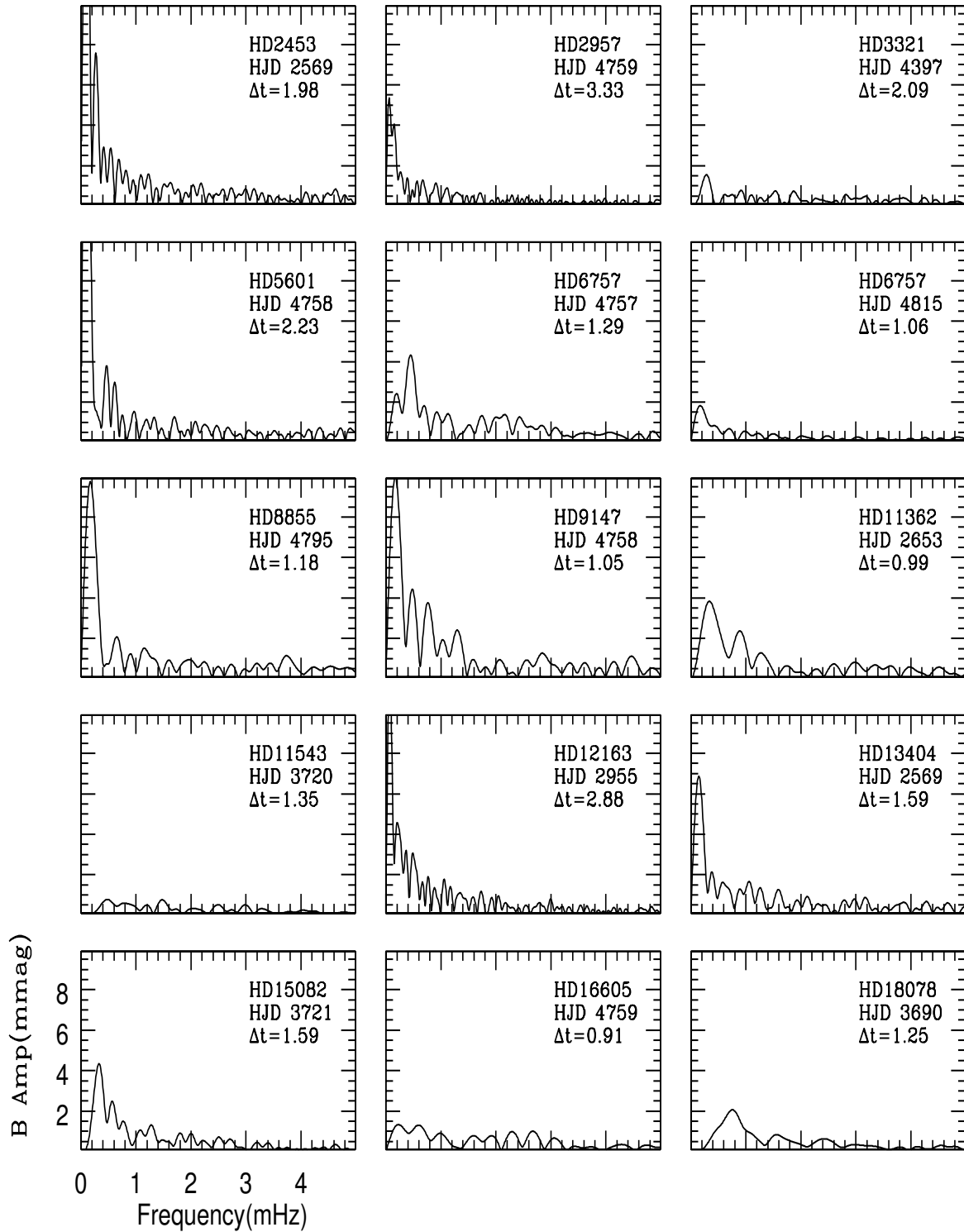


Fig. 11 : Null results from the Nainital-Cape survey: Examples of amplitude spectra for sample stars corrected only for extinction, and in some cases for some very long-term sky transparency variations. Each panel contains the Fourier transform of an individual light curve, covering a frequency range of 0 to 5 mHz, and an amplitude range of 0 to 9 mmag. The name of the object, date of the observation in Heliocentric Julian date (HJD 245000+) and duration of the observations in hours (hr), are mentioned in each panel.

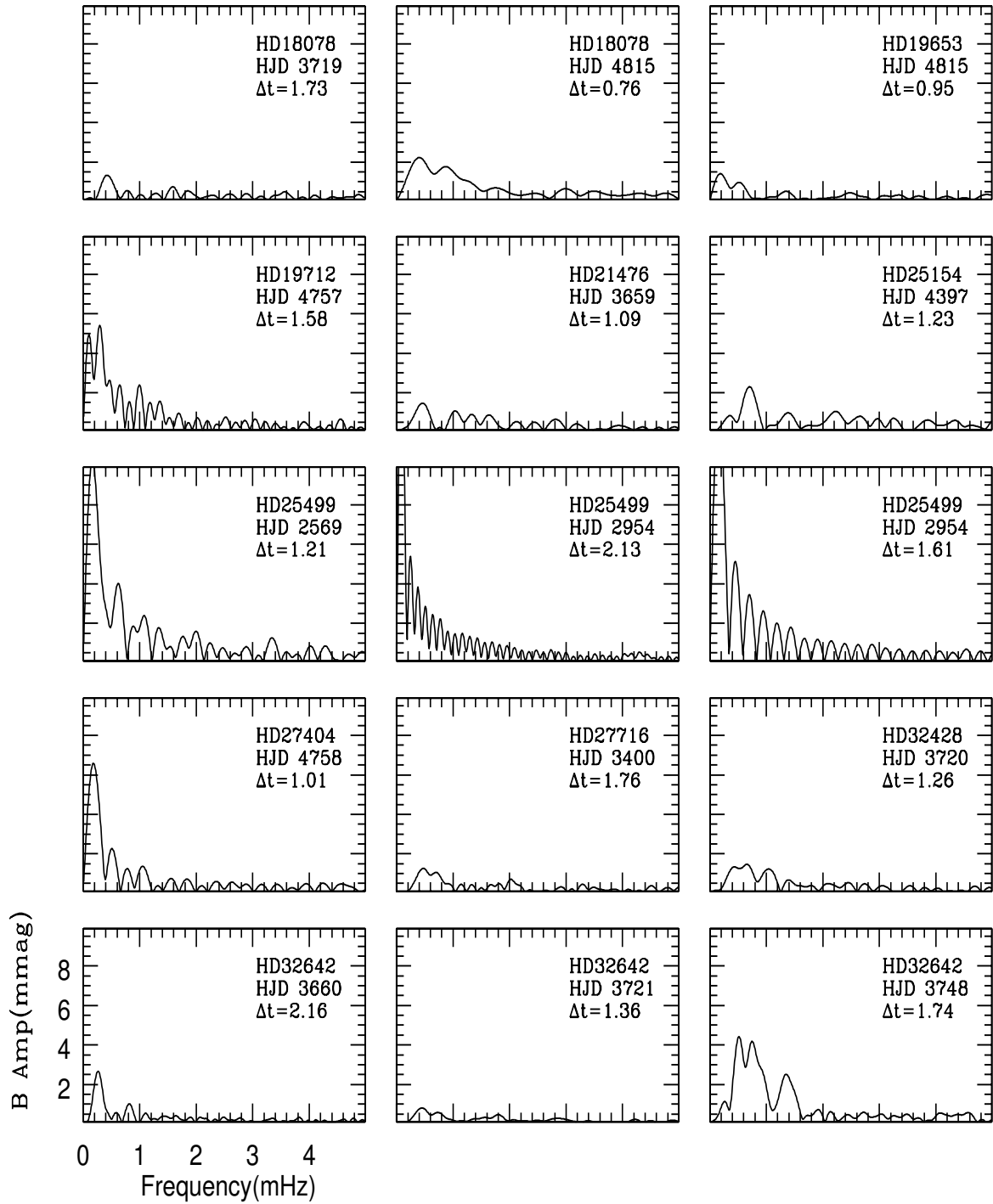


Fig. 11 : Cont.

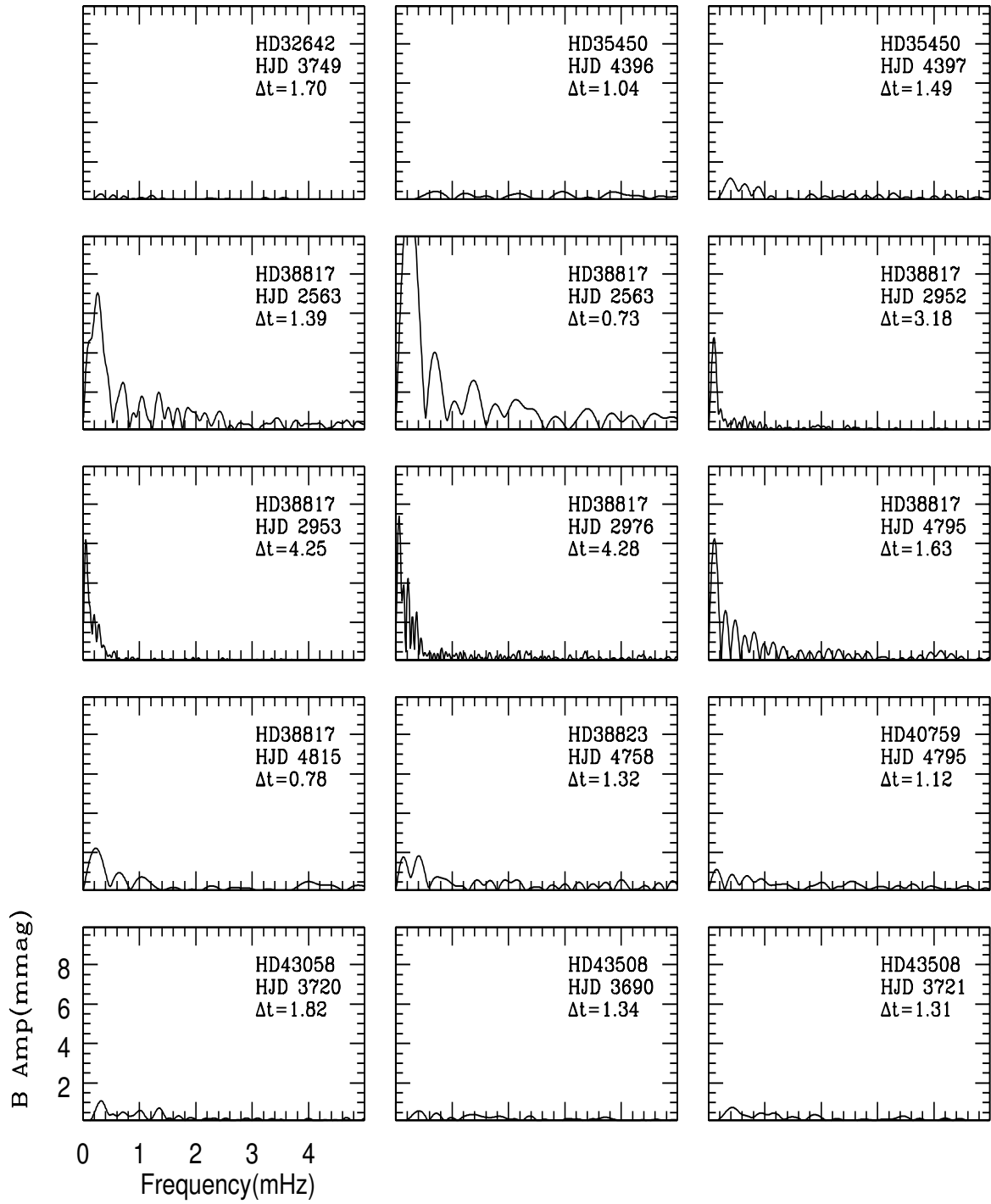


Fig. 11 : Cont.

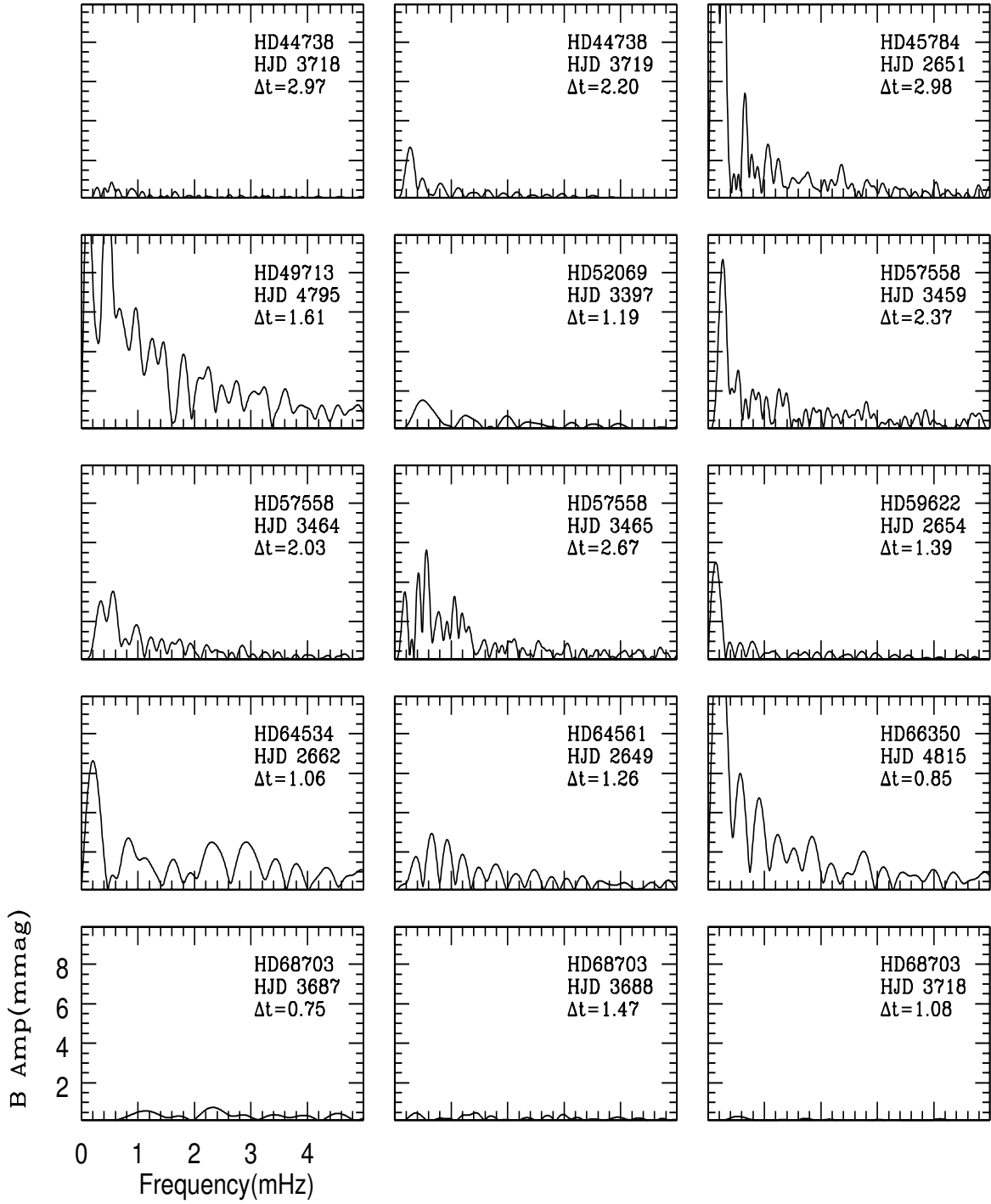


Fig. 11 : Cont.

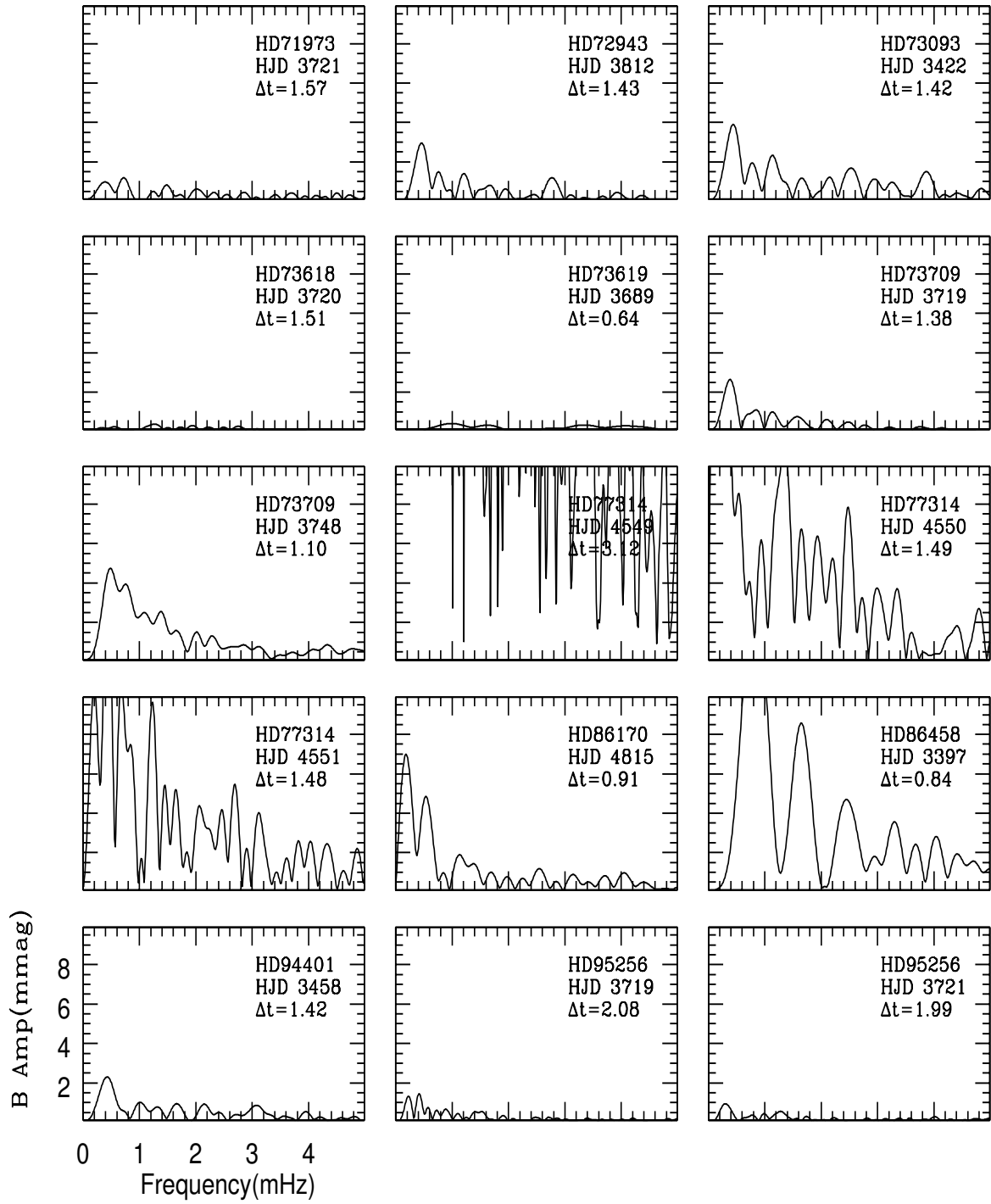


Fig. 11 : Cont.

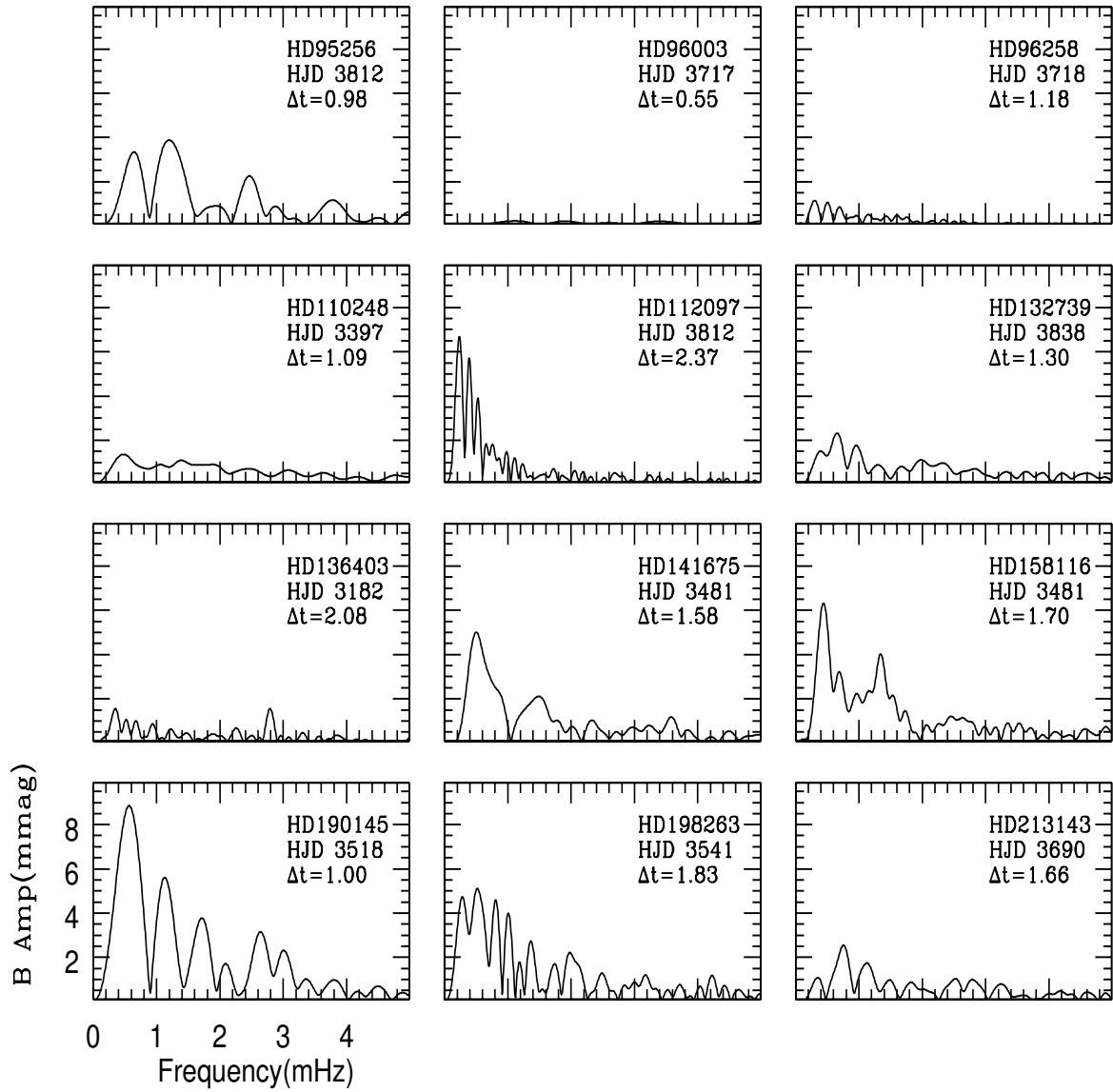


Fig. 11 : Cont.

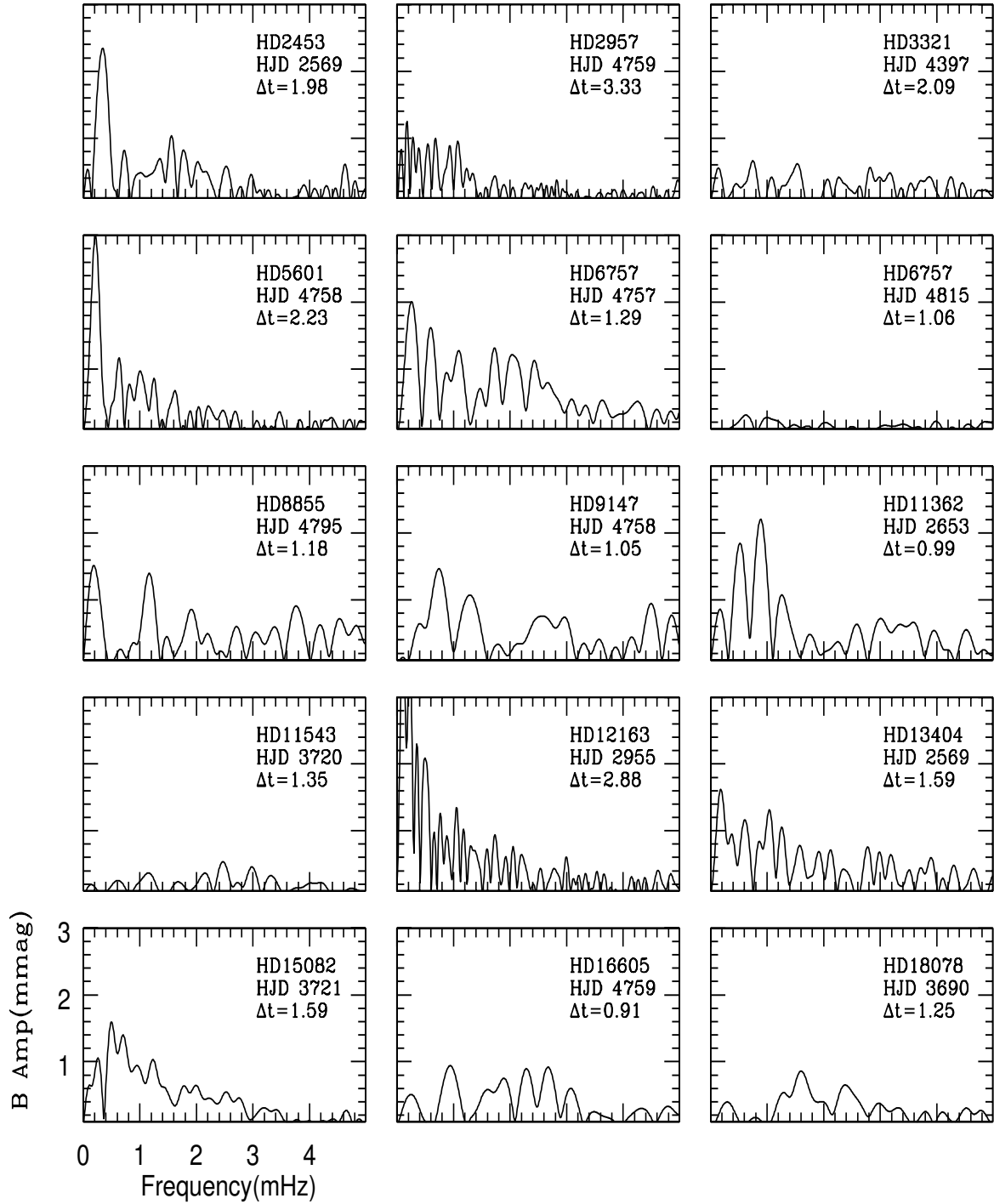


Fig. 12 : Null results from the Nainital-Cape survey: Examples of prewhitened amplitude spectra for sample stars. Each panel contains the Fourier transform of an individual light curve, covering a frequency range of 0 to 5 mHz, and an amplitude range of 0 to 3 mmag. The name of the object, date of the observation in Heliocentric Julian date (HJD 245000+) and the length duration in hours (hr), are mentioned in each panel.

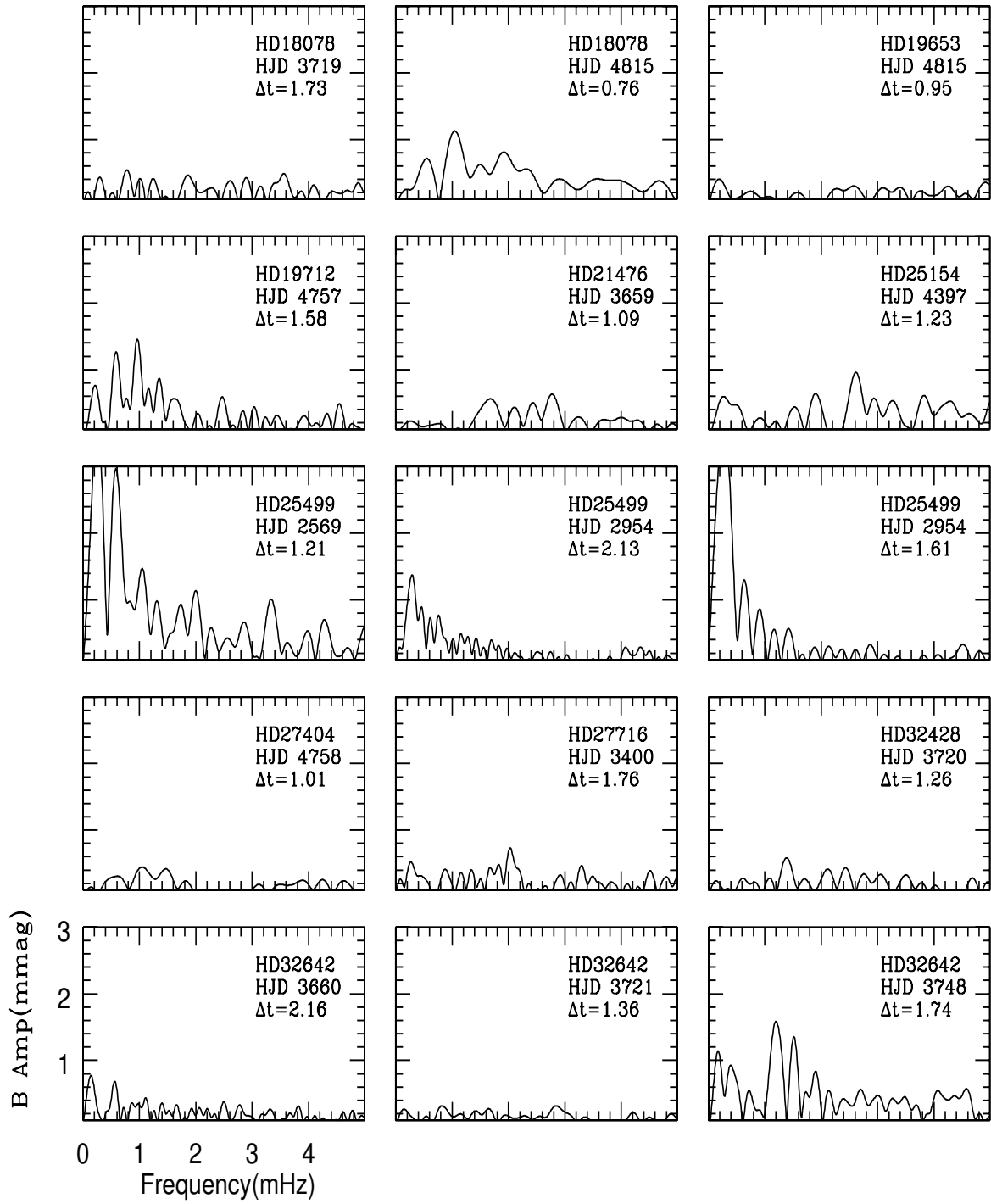


Fig. 12 : Cont.

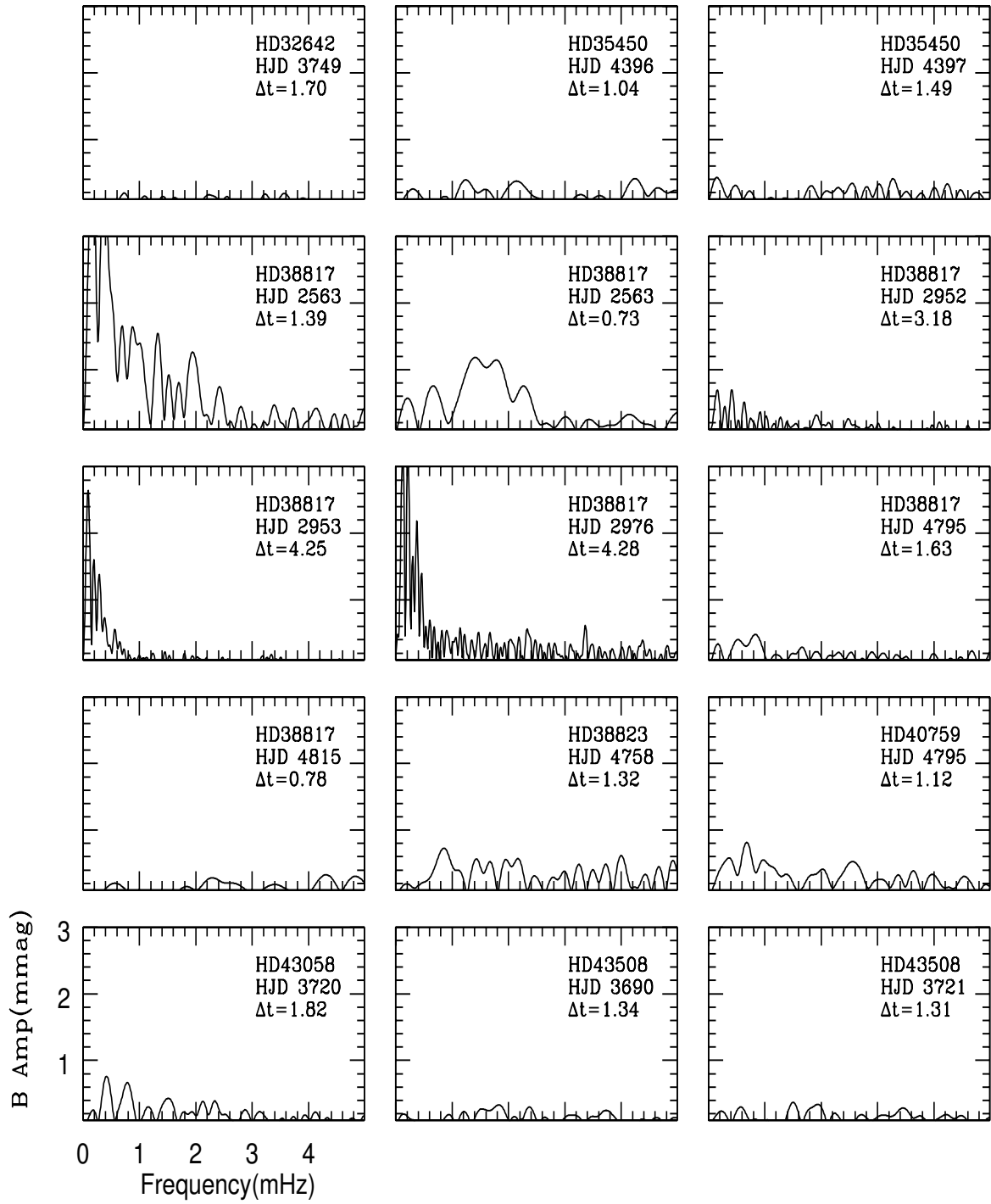


Fig. 12 : Cont.

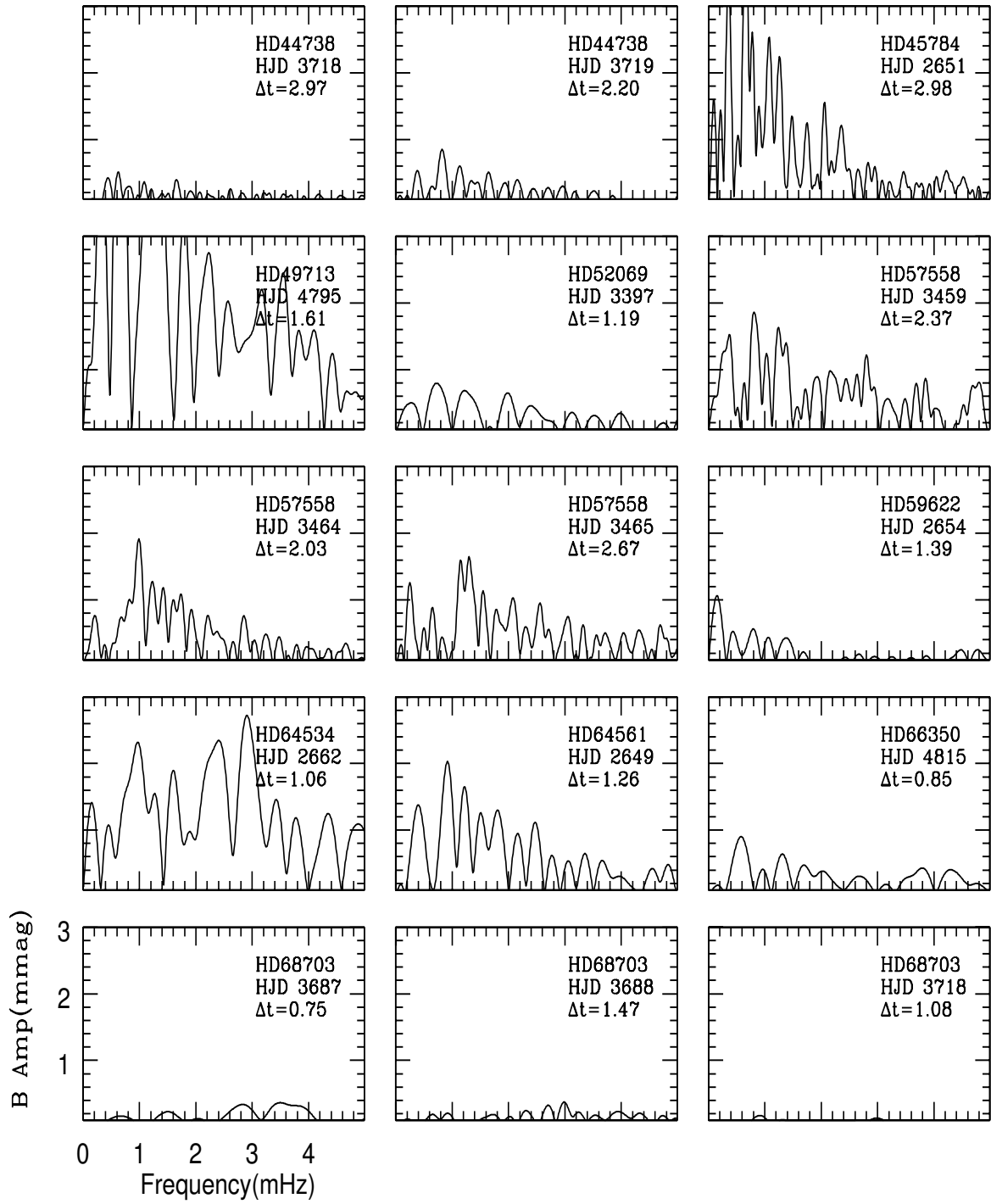


Fig. 12 : Cont.

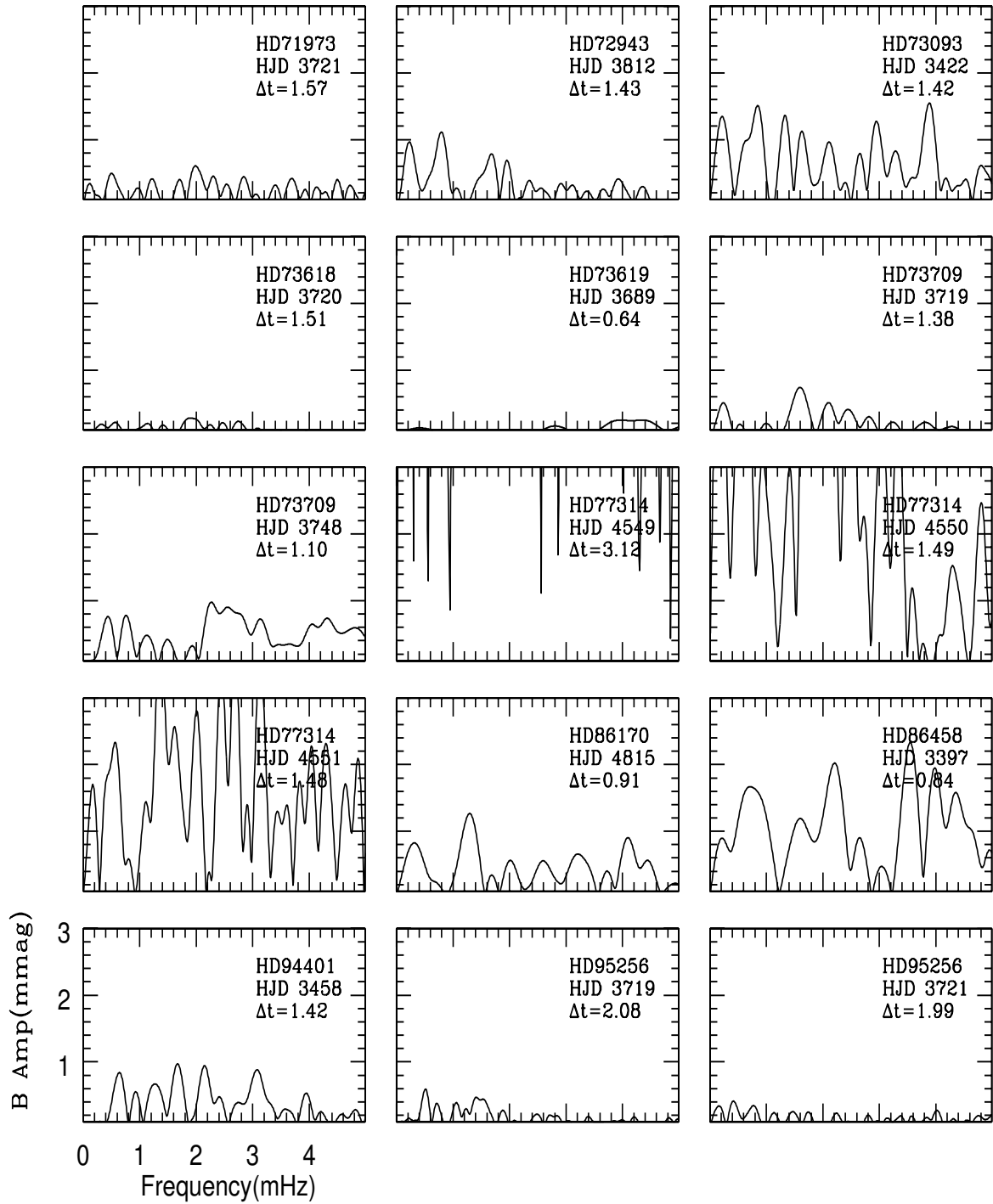


Fig. 12 : Cont.

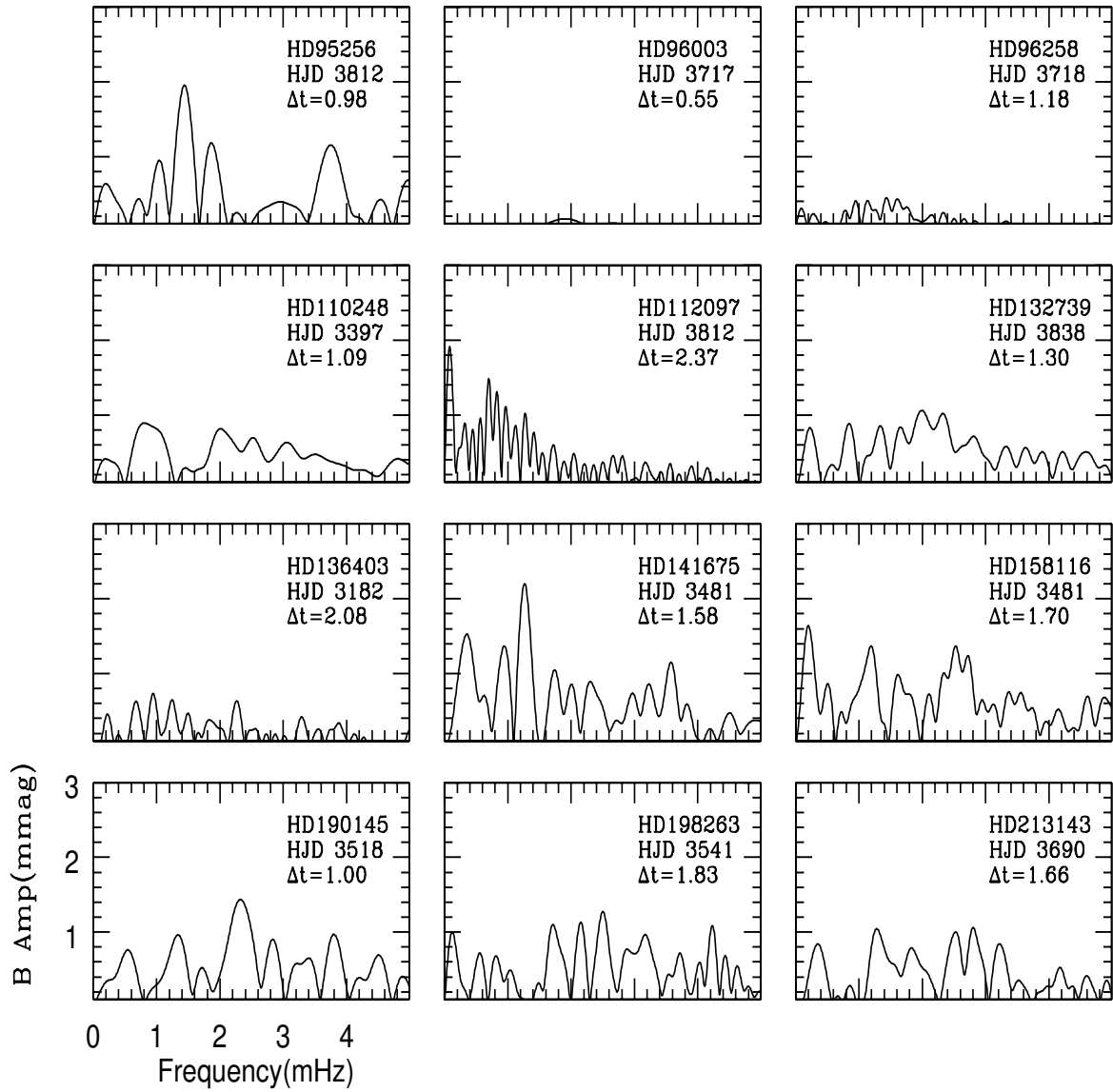


Fig. 12 : Cont.

